

# **DESIGN AND DEVELOPMENT OF FRACTAL MICROSTRIP ANTENNA ARRAYS FOR MIMO APPLICATIONS**

*A Thesis submitted in partial fulfillment of the requirements for the award of Degree  
of*

**MASTER OF ENGINEERING  
In  
WIRELESS COMMUNICATION**

Submitted By

**SHEIFALI GUPTA**

**Roll No. 801463024**

Under guidance of

**Mrs. AMANPREET KAUR**

Assistant Professor, ECED

T.U, Patiala



**Department of Electronics and Communication Engineering  
THAPAR UNIVERSITY, PATIALA  
(Declared as Deemed-to-be University u/s of the UGC Act, 1956)  
June 2016**

## CANDIDATE'S DECLARATION CERTIFICATE

I hereby certify that the work which is being presented in the Project entitled “**Design and Development of Fractal Microstrip Antenna Arrays for MIMO Applications**” in partial fulfilment of requirement for the award of degree of ME (Wireless Communications) at Thapar University, Patiala, is my own work carried out under the supervision of **Dr. Amanpreet Kaur** (Assistant Professor), **ECED** during 4<sup>th</sup> semester, 2015-2016.

Date: 13/7/16

  
**Sheifali Gupta**

801463024

This is to certify that the above statement made by the candidate is connect to the best of my knowledge.

Date: 13/7/16

  
**Dr. Amanpreet Kaur**

Assistant Professor

ECED

Countersigned by:

  
**Dr. Sanjay Sharma**

Professor & Head

ECED , Department

  
**(Dr. S.S Bhatia)**

Dean of Academic Affairs

Thapar University

Patiala-147004

## **ACKNOWLEDGEMENT**

First of all, I would like to express my gratitude to **Dr. Amanpreet Kaur**, Electronics and Communication Engineering Department, Thapar University, Patiala for her patient guidance and support throughout this report. I am truly very fortunate to have the opportunity to work with her. I found her guidance to be extremely valuable.

I am also thankful to our **Head of the Department, Dr. Sanjay Sharma** for providing me adequate environment in carrying the work. I would like to extend my gratitude to entire faculty and staff of Electronics and Communication Engineering Department who directly or indirectly helped me in the process and contributed towards this work.

Finally, I would like to thank my parents for their years of unyielding love and encouragement. I admire their support and sacrifice.

*Sheifali*  
**Sheifali Gupta**

801463024

## **ABSTRACT**

During last two decades, significant advancement is seen in wireless communication. To fulfil the increasing demands of users around the world higher data rate in in RF wireless communication system. It indicates that bandwidth enhancement is the main concern in the antenna design. In addition, compactness of design is equally important to place our antenna system easily in the modern communication devices.

In the work presented, transmission line model is used for the simulation and analysis of slotted rectangular and triangular shaped patch microstrip antenna using feed line method. The reason behind this is to study the various parameters such as impedance bandwidth, radiation pattern and return loss of the presented antenna structure.

Conducting patch with triangular shape is preferred due to the improved results over the rectangular patch antenna especially in the antenna arrays. Selection of length and width of the patch is very crucial parameter along with the dimensions of feed line.

So in this thesis, a complementary sierpinksi gasket fractal antenna array for MIMO systems is designed at resonating frequency of 4.83 GHz, with the bandwidth of 408.2 MHz for WLAN application using CST Microwave Studio 10. Various parameters affecting the performance of MIMO antenna array such as envelope correlation coefficient, diversity gain are studied and physical parameters such as slot in the patch & DGS are also considered with its fabrication done.

Also Compact triangular Patch microstrip fractal antenna array with defected ground structure is designed at resonating frequency of 5.6GHz, covering band 5.43-5.84GHz giving bandwidth of 418MHz for WLAN application. Second order fractals are made in patch with optimised slot in ground plane, fabrication for this design is also done. Antenna parameters like ECC, diversity gain, bandwidth, return loss are determined.

Both the fabricated wide band antennas are tested using VNA model no: E5071C. The testing results are shown along with the comparison between the simulated results and fabricated results. The operating frequency of single wide band at 4.83GHz and 5.6GHz is obtained at 4.38GHz and 5.45GHz respectively, also the range of frequencies covered by band has shifted to left side.

## LIST OF CONTENT

Content	Page No.
<i>CERTIFICATE</i>	<i>i</i>
<i>ACKNOWLEDGEMENT</i>	<i>ii</i>
<i>ABSTRACT</i>	<i>iii</i>
<i>CONTENTS</i>	<i>iv</i>
<i>LIST OF ABBREVIATIONS</i>	<i>vii</i>
<i>LIST OF FIGURES</i>	<i>viii</i>
<i>LIST OF TABLES</i>	<i>xi</i>
<b>1. Introduction</b>	<b>1</b>
1.1. Wireless Communication	1
1.2. Multiple Input Multiple Output(MIMO)	2
1.2.1. Multiple Input Multiple Output(MIMO)Basics	2
1.2.2. MIMO Configurations	2
1.2.2.1. MIMO-SISO	4
1.2.2.2. MIMO-SIMO	4
1.2.2.3. MIMO-MISO	4
1.2.2.4. MIMO	5
1.2.3. Fading Channels	5
1.2.4. MIMO Channel Model	5
1.3. Need for Antennas	8
1.3.1. Types of Antennas	9
1.3.2. Introduction of Microstrip Patch Antenna	10
1.3.3. Basic Characteristics of MSA Operation	10
1.3.4. Transmission Line Model	11
1.3.5. Feeding Techniques	13
1.3.5.1. Microstrip Line Feeding	13
1.3.5.2. Coaxial Feeding	13
1.3.5.3. Aperture Coupling	14
1.3.5.4. Proximity Coupling	14
1.4. Numerical Analysis of Microstrip Antennas	15

1.4.1. Finite Difference Time Domain Technique (FDTD)	16
1.4.2. Theoretical Analysis of FDTD Method	18
1.4.3. FDTD Gridding Structure	20
1.5. Research Gaps	20
1.6. Objective of Thesis	20
1.7. Thesis Organization	
<b>2. Literature Survey</b>	<b>22</b>
2.1. Microstrip Antenna	23
2.2. Microstrip Feed Antennas with different geometries	24
2.3. Triangular Patch Microstrip Antennas	27
2.4. MIMO Antenna Arrays	27
<b>3. Single Band Microstrip Antenna Design for WLAN Applications</b>	<b>31</b>
3.1. Design of Single Band Slotted Rectangular Patch Microstrip Antenna at 5.2 GHz	31
3.1.1. Simulation Setup and Results	32
3.1.1.1. Return Loss and Antenna Bandwidth	33
3.1.1.2. Smith Chart and Antenna Impedance	33
3.1.1.3. Directivity	34
3.1.1.4. Current Distribution	34
3.2. Design of Single Band Slotted Triangular Patch Microstrip Antenna at 4.8 GHz	34
3.2.1. Simulation Setup and Results	35
3.2.1.1. Return Loss and Antenna Bandwidth	36
3.2.1.2. Smith Chart and Antenna Impedance	36
3.2.1.3. Directivity	37
3.2.1.4. Current Distribution	37
<b>4. Wide Band Microstrip Antenna Design for WLAN Applications</b>	<b>39</b>
4.1. Design of Complementary Sierpinski Gasket Fractal Antenna Array for MIMO Applications with Defected Ground Structure	39
4.1.1. Simulation Setup and Results	40
4.1.1.1. Return Loss and Antenna Bandwidth	

4.1.1.2. Smith Chart and Antenna Impedance	40
4.1.1.3. Directivity	41
4.1.1.4. Current Distribution	42
4.1.1.5. MIMO Parameters	42
4.1.1.5.a. Envelope Correlation Coefficient	43
4.1.1.5.b. Diversity Gain	44
4.1.1.5.c. Capacity Analysis	45
4.2 Design of Compact Triangular Microstrip Patch Fractal Antenna Array with Defected Ground Structure for MIMO Applications	46
4.2.1. Simulation Setup and Results	47
4.2.1.1. Return Loss and Antenna Bandwidth	48
4.2.1.2. Smith Chart and Antenna Impedance	49
4.2.1.3. Directivity	49
4.2.1.4. Current Distribution	50
4.2.1.5. MIMO Parameters	50
4.2.1.5.a. Envelope Correlation Coefficient	50
4.2.1.5.b. Diversity Gain	50
4.2.1.5.c. Capacity Analysis	51
<b>5. Fabrication and Testing of Proposed MSA</b>	<b>54</b>
5.1. Fabrication Process	55
5.2. Instruments used for Fabricating a Microstrip Patch Antenna	56
5.3. Fabricated Antennas at Frequency 4.8 GHz and 5.6 GHz	58
5.4. Testing of Antennas on VNA	59
5.4.1 Simulated and Measured Results of Antenna Arrays	59
5.4.2. Discussion of results	
<b>6. Conclusion and Future Work</b>	<b>62</b>
6.1. Conclusions	63
6.2. Future Work	
<b>List of Publications</b>	<b>64</b>
<b>References</b>	<b>65</b>

## List of Abbreviation

WLAN	Wireless Local Area Network
SISO	Single Input Single Output
SIMO	Single Input Multiple Output
MISO	Multiple Input Single Output
MIMO	Multiple Input Multiple Output
BC	Broadcast Channel
LTE	Long Term Evolution
OFDM	Orthogonal Frequency Division Multiple
WIFI	Wireless Fidelity
WiMAX	Worldwide Interoperability for Microwave
GPS	Global Positioning System
MSA	Microstrip Antenna
FDTD	Finite Difference Time Domain
CST MWS	Computer Simulation Tool Microwave Studio
RF	Radio Frequency
DGS	Defected Ground Structure
ECC	Envelope Correlation Coefficient
EBG	Electromagnetic Band Gap

## LIST OF FIGURES

<b>Figure No.</b>	<b>Figures</b>	<b>Page No.</b>
Figure1.1.	Block Diagram of MIMO System	3
Figure1.2.	SISO System	4
Figure1.3.	SIMO System	5
Figure1.4.	MISO System	6
Figure1.5.	MIMO System	6
Figure1.6.	Microstrip Patch Antenna	10
Figure1.7.	Physical and Effective Length of Microstrip Patch Antenna	12
Figure1.8.	(a)Microstrip Feeding, (b) Microstrip line with Inset	13
Figure1.9.	Coaxial Feeding	14
Figure1.10.	Aperture Coupling	14
Figure1.11.	Proximity Coupling	15
Figure1.12.	Leap Frog Algorithm	16
Figure1.13.	Field Calculation Points	17
Figure1.14.	FDTD Gridding Scheme	18
Figure1.15.	Intersection of PMC for slot 3 representing slanted edge of the antenna	19
Figure3.1.	Front View of U-slot Rectangular Patch Microstrip Antenna	32
Figure3.2.	Return Loss $S_{11}$ (dB) Versus Frequency Plot of the Single band U-slot Antenna	32
Figure3.3.	Smith Chart Showing the Characteristics Impedance of Single band U-slot Antenna	33
Figure3.4.	3D Radiation Pattern of the Directivity of the Single band U-slot Antenna	33
Figure3.5.	Surface Current Distribution of the Single band U-slot Antenna	34
Figure3.6.	Front View of Slotted Triangular Patch Microstrip	35

	Antenna	
Figure3.7.	Return Loss $S_{11}$ (dB) Versus Frequency Plot of the Single band Slotted Triangular Patch Antenna	36
Figure3.8.	Smith Chart Showing the Characteristics Impedance of Single band Slotted Triangular Patch Antenna	36
Figure3.9.	3D Radiation Pattern of the Directivity of the Single band Slotted Triangular Patch Antenna	37
Figure3.10.	Surface Current Distribution of the Single band Slotted Triangular Patch Antenna	37
Figure4.1.	Wide Band Complementary Sierpinski Gasket Fractal Antenna Array (a)Front View Showing Fractal Design in Patch, (b)Back View Showing DGS	40
Figure4.2.	Return Loss $S_{11}$ (dB) Versus Frequency Plot of Wide Band Complementary Sierpinski Gasket Fractal Antenna Array	41
Figure4.3.	Smith Chart Showing the Characteristics Impedance of Wide Band Complementary Sierpinski Gasket Fractal Antenna Array	41
Figure4.4.	Wide Band Complementary Sierpinski Gasket Fractal Antenna Array (a) 3D Radiation Pattern of the Directivity due to excitation port 1, (b) 3D Radiation Pattern of the Directivity due to excitation port 2	42
Figure4.5.	Surface Current Distribution of Wide Band Complementary Sierpinski Gasket Fractal Antenna Array (a) due to excitation port 1, (b) due to excitation port 2	43
Figure4.6.	Envelope Correlation coefficient of Wide Band Complementary Sierpinski Gasket Fractal Antenna Array	44
Figure4.7.	Diversity Gain of Wide Band Complementary Sierpinski Gasket Fractal Antenna Array	44
Figure4.8.	Capacity versus Bandwidth plot	45
Figure4.9.	Wide Band Compact Triangular Microstrip Patch Fractal Antenna Array (a)Front View Showing Fractal Design in Patch, (b)Back View Showing DGS	46
Figure4.10.	Figure 4.10(a)Return Loss $S_{11}$ (in dB) of Simulated First Order Fractal Antenna (b) Return Loss $S_{11}$ (dB)	47

	versus Frequency Plot of Compact Triangular Microstrip Patch Fractal Antenna Array	
Figure4.11.	Smith Chart Showing the Characteristics Impedance of Compact Triangular Microstrip Patch Fractal Antenna Array	48
Figure4.12.	Wide Band Compact Triangular Microstrip Patch Fractal Antenna Array (a) 3D Radiation Pattern of the Directivity due to excitation port 1, (b) 3D Radiation Pattern of the Directivity due to excitation port 2	48-49
Figure4.13.	Surface Current Distribution of Compact Triangular Microstrip Patch Fractal Antenna Array (a) due to excitation port 1, (b) due to excitation port 2	49-50
Figure4.14.	Envelope Correlation coefficient of Compact Triangular Microstrip Patch Fractal Antenna Array	50
Figure4.15.	Diversity Gain of Compact Triangular Microstrip Patch Fractal Antenna Array	51
Figure4.16.	Capacity versus bandwidth plot	51
Figure5.1.	Fabrication Flow of PCB Design	54-55
Figure5.2.	PCB Cutter	55
Figure 5.3.	PCB Coating Unit	56
Figure.5.4.	Oven Unit	56
Figure.5.5.	Etching Unit	56
Figure 5.6.	(a) Patch with Microstrip Feed Line (b) DGS on Ground Plane	57
Figure 5.7.	(a) Patch with Microstrip Feed Line (b) DGS on Ground Plane	57
Figure 5.8.	Instrument used for Testing	58
Figure 5.9.	Return Loss $S_{11}$ (dB) Versus Frequency Plot of Simulated Antenna at 4.83GHz	58
Figure 5.10.	Return Loss $S_{11}$ (dB) Versus Frequency Plot of Simulated Antenna at 5.6GHz	59
Figure 5.11.	Return loss (a),(b)Tested results at 4.38GHz	59
Figure 5.12.	Transmission loss (a),(b)Tested results at 5.45GHz	60

## LIST OF TABLES

<b>Table No.</b>	<b>Tables</b>	<b>Page No.</b>
Table.3.1.	Design Specifications of Single Band U-Slot Rectangular Patch Microstrip Antenna	31
Table.3.2.	Optimized Dimensions of Single Band U-Slot Rectangular Patch Microstrip Antenna	31
Table.3.3.	Design Specifications of Single Band Slotted Triangular Patch Microstrip Antenna	35
Table.3.4.	Optimized Dimensions of Single Band Slotted Triangular Patch Microstrip Antenna	35
Table.4.1.	Design Specifications of Wide Band Complementary gasket fractal Antenna Microstrip Antenna Array	39
Table.4.2.	Optimized Dimensions of Wide Band Complementary gasket fractal Antenna Microstrip Antenna Array	39
Table.4.3.	Design Specifications of Wide Band Compact Triangular patch fractal Antenna Array	46
Table.4.4.	Optimized Dimensions of Wide Band Compact Triangular patch fractal Antenna Array	46
Table.5.1.	Comparison between Simulated results and fabricated results	60
Table.5.2.	Comparison between Simulated results and fabricated results	61
Table.6.1.	Concluded results of the designs	63

## **Chapter 1**

### **Wireless Communication**

---

Communication is the process of exchanging information between two distinct points. In earlier days communication between two distant stations was made possible using devices like drums, some visible methods like, smoke signals and signal flags. With the advancement of the technology, the electromagnetic spectrum was utilized and used for long distance communication. When EM spectrum is being utilized for long distance communication which was made possible without using wires, it is called wireless communication.

#### **1.1 Wireless Communication**

During 19<sup>th</sup> century, the term wireless communication was introduced and this technology has developed over the subsequent years. It is one of the most important mediums of transmission of information from one device to the other using RF waves for communication. Some currently used wireless technologies are the Bluetooth Technology, Zig bee , GPS, Wi-Fi. Also nowadays wireless phones are there which include 3G and 4G networks, Bluetooth and Wi-Fi technologies [1].

#### **Advantages of Wireless Communication**

A few advantages of wireless communication make it a preferred choice amongst users.

- Installation and Maintenance cost is very less.
- Any information or data can be transferred anywhere with very high speed.
- In remote areas this is very helpful for workers, doctors so that they can be in touch with other people.

#### **Disadvantages of Wireless Communication**

- Wireless signals can be easily captured by an unauthorized person through the air.
- Wireless signals are sometimes subjected to multipath and fading.

In Wireless channel, signal to noise ratio is affected by fading and error rate gets affected, after transmission of digital data. In order to overcome the effects of fading diversity

principle is used to provide replicas of the same signal at the receiver side. If all these are made to be affected in different ways by the signal path, the probability of getting affected at the same time is considerably reduced. In this way diversity helps in link stability and improvement in performance, reducing error rate [1].

Different diversity schemes provide various advantages in improving the performance of existing wireless communication systems. These can be implemented in the following ways to improve the quality of output obtained at the receiver.

- **Time diversity:** In this scheme transmission of message takes place at different times, so different time slots and channel coding is used.
- **Frequency diversity:** In this we use different frequencies by using technologies such as spread spectrum / OFDM or different channels.
- **Space diversity:** Antennas located in different directions are used to take advantage of the different radio paths. Out of all the mentioned diversity schemes, the most popularly used one is a space diversity system.

## **1.2 Multiple Input Multiple Output (MIMO) Development and History**

Arogyaswami Paulraj and Thomas Kailath proposed in 1993, the use of spatial multiplexing using MIMO and in the next year their US patent was granted. In 1998, Bell Labs first demonstrated a laboratory prototype of spatial multiplexing. MIMO systems were based on basic spatial diversity where the system was used to limit the degradation caused due to multipath propagation. Then utilization of the multipath propagation started and additional signal paths are to be considered as extra channels to carry additional data.

### **1.2.1 MIMO -Multiple Input Multiple Output basics**

Space-time signal processing is one of the main ideas behind MIMO systems which complements the time with the spatial dimension inherent for using multiple antennas which should be spatially distributed, i.e. using multiple antennas at different locations. Therefore these systems can be viewed as an extension to be used as smart antennas to improve wireless.

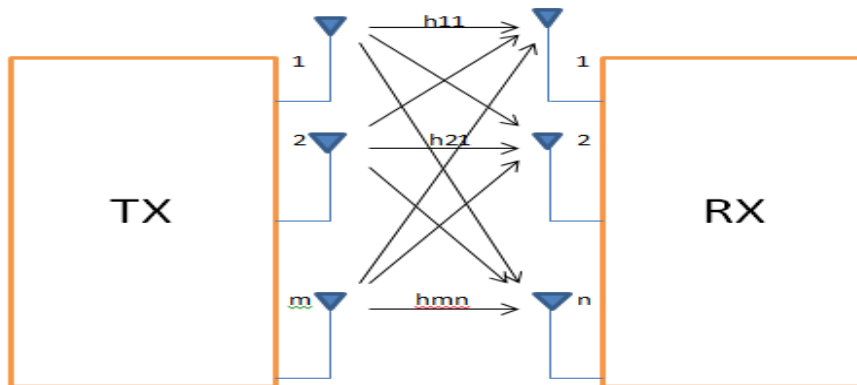


Figure1.1 General Representation of MIMO system

Figure 1.1 shows a typical space diversity system with multiple numbers of transmitter as well as the receiver antennas in a MIMO system. From transmitter to receiver, signal can take different routes to travel; therefore by moving antennas to a small distance will change their routes. Various routes are available for the number of objects appearing to the side or directly in the path of transmitted and received signals. These multiple routes were only for the introduction of interference. Nowadays by using MIMO, advantage can be taken from these additional paths. Therefore after enhancing the SNR or improving the link capacity additional robustness to the radio link can be provided.

The two main forms for MIMO (Multiple Input Multiple Output) are explained below:

- **Spatial diversity:** Spatial diversity often refers to transmit and receive diversity. To improve system reliability with respect to the various forms of fading, the signal to noise ratio can be improved.
- **Spatial multiplexing:** It is the form of MIMO in which utilization of the different paths to carry extra traffic, i.e. increasing the data throughput capability to provide extra data capacity is made.

MIMO wireless technology increases the channel capacity by using multiple antennas and obeying Shannon's law. For the linear increase in the throughput of the channel taking help of every antenna pair added to the system, the number of receive and transmit antennas should be increased. This makes MIMO wireless technology a very important wireless technique in recent years. Available bandwidth needs to be used very effectively because

spectral bandwidth is important for radio communications systems. MIMO wireless technology has made a place in one of these techniques [2].

### 1.2.2 MIMO Configurations - SISO, SIMO, MISO, MU-MIMO

There are various forms of multiple input multiple output system configurations available. These are SISO (Single Input Single Output), SIMO (Single Input Multiple output), MISO (Multiple Input Single Output) and MIMO (Multiple Input multiple Output). These different configurations have number of advantages and disadvantages - which can be compensated for optimum result for any specific application. Different forms of MIMO systems are - SISO, SIMO, MISO and MIMO. These require different numbers of transmitters and receivers, hence have different levels of complexity. Different antenna technologies refer to single or multiple inputs and outputs, related to the radio link. So, the input is given to transmitter so that it transmits into the link or signal path, and the output is received at receiver which is output of the wireless link.

#### 1.2.2.1 MIMO – SISO

SISO - Single Input Single Output is the elementary form of wireless radio link defined in MIMO. This is standard effective radio channel - with single antenna present at the transmitter and single at the receiver side. No diversity gain is there and no requirement for additional processing.

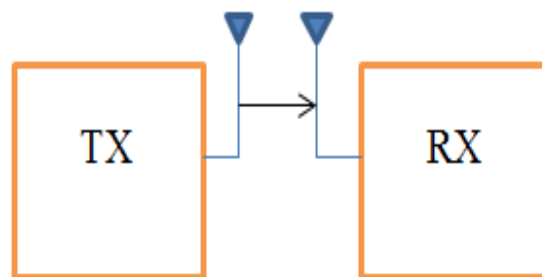


Figure1.2 SISO - Single Input Single Output

SISO system is simplest in all and it does not require processing. It has its own limitations in the terms of performance. SISO system will have more impact of interference and

fading than a MIMO system and the channel bandwidth is limited by Shannon's law - the throughput is dependent on the channel bandwidth and the signal to noise ratio [1].

### 1.2.2.2 MIMO – SIMO

When there is single transmitter antenna and multiple receiver antennas the configuration is known as SIMO. It is also a form of receive diversity. In this system the receiver receives signals from a number of individual sources to combat fading. It has been used for many years to overcome the effects of ionospheric interference and fading.

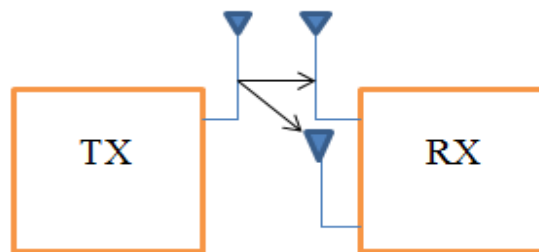


Figure1.3. SIMO - Single Input Multiple Output

Advantage of SIMO is that it is quite easy in implementation in spite of various drawbacks such as the requirement of processing in the receiver. Using a SIMO is accepted for many applications, but when the location receiver is a mobile device such as a cellphone handset, processing levels depends on size, cost and drainage of battery.

Two forms of SIMO that can be used:

- **Switched diversity SIMO:** This SIMO form searches for the strongest signal and switch that signal to antenna.
- **Maximum ratio combining SIMO:** Both signals are taken and summed by multiplying each by its channel weight to give combination. In this way, contribution is made by the signals from both antennas.

### 1.2.2.3 MIMO - MISO

MISO (Multiple Input Single Output) is a form of transmit diversity. In this case, the same data is transmitted from the two different transmitter antennas. The receiver will then receive the best possible signal which can be use by it further to extract the required data.

Significant advantage of MISO system is the reduced level of processing required for redundancy coding at the receiver. There occurs a positive impact regarding size, cost and battery life of system, there is need of less battery consumption at the lower processing level.

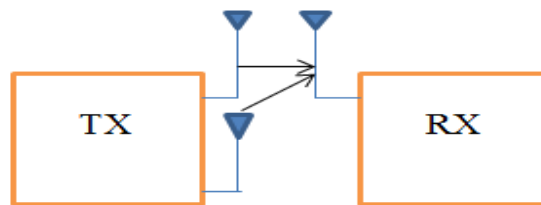


Figure1.4. MISO - Multiple Input Single Output

#### 1.2.2.4 MIMO

Where there are multiple antennas at both the transmitter and receiver end of the radio link, this is called as MIMO - Multiple Input Multiple Output. MIMO provides improved robust channel and its throughput.

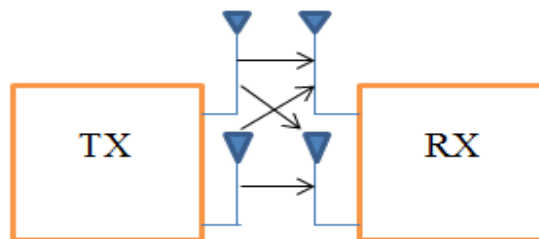


Figure1.5. MIMO - Multiple Input Multiple Output

**1.2.3 Fading Channels** The environment in which these diversity systems are used can be varying. Depending upon the density of scatters & line of sight path, these are classified as under:

- **Rayleigh fading channel**

It describes envelope distribution of received signal for all the components which are present in non-line of sight [1], [2]. This fading assumes that signals at receiving side have large number of reflected waves which are independent and identically distributed in terms of phase and quadrature amplitudes. The wireless radio

frequency channel is distinguished by multipath signals. The signal at the receiver side contains not only a direct line-of-sight (LOS) signal, also a large number of reflected signals. These reflected signals interfere with the direct signal, due to which there occurs a significant deterioration in the system performance. Also, when antenna moves, there occurs channel variation with respect to location and time, because reflected signals with relative phases leads to variations in time of the receiver's amplitude and phase which means fading.

- **Ricean Fading Channel**

This fading is quite same as Rayleigh fading, except that Ricean fading has a robust LOS component. A Ricean model also considers the following:

- i. The prevalent signal is a phasor sum of two or more prevalent signals, e.g. ground reflection, plus the line-of-sight. Then this combined signal is mainly treated as a passive process,
- ii. The prevalent signal can also be used to attenuate shadow.

- **Nakagami Fading Channel**

This fading occurs for multiple signal scattering with different clusters of reflected signals with relatively large delay-time spreads. Within a cluster, the delay times are approximately equal for all signals, but the phases are random for individual reflected signals. Therefore the envelope of each added cluster signal has Rayleigh distribution. There is the difference in the average time delay between clusters. When the delay time is greater than the duration of bit, the different clusters generates serious inter-symbol interference (ISI).

Depending upon the type of environment a wireless modelling system selects a respective fading channel & uses a channel matrix to describe the kind of output that can be obtained.

#### **1.2.4 MIMO Channel Model**

For multiple antennas at both the receiver and the transmitter sides (Fig.1), the multiple inputs and multiple outputs is exhibited by the channel and its capacity is determined by the extension of Shannon's capacity formula, which is given below. An antenna array is

present with  $n_t$  elements at the transmitter side and with  $n_r$  elements at the receiver side. The impulse response of the channel between the  $j^{\text{th}}$  transmitter element and the  $i^{\text{th}}$  receiver element is denoted as  $h_{i,j}(\tau, t)$ . The MIMO channel is then given by the  $n_r \times n_t$   $H(\tau, t)$  matrix:

$$H(\tau, t) = \begin{bmatrix} h_{11}(\tau, t) & h_{12}(\tau, t) & \dots & h_{1n}(\tau, t) \\ h_{21}(\tau, t) & h_{22}(\tau, t) & \dots & h_{2n}(\tau, t) \\ \cdot & \cdot & \dots & \cdot \\ \cdot & \cdot & \dots & \cdot \\ h_{m1}(\tau, t) & h_{m2}(\tau, t) & \dots & h_{mn}(\tau, t) \end{bmatrix}$$

The elements present in the matrix are complex numbers which correlates with the phase shift and attenuation in the wireless channel that leads to the signal reaching at the receiving end with delay  $\tau$ . The input-output relationship for the MIMO system is given in the below equation:

$$y(t) = H(\tau, t) * s(t) + u(t) \quad (1.1)$$

where symbol  $*$  means convolution,  $s(t)$  is a vector  $n_t \times 1$  corresponds to the  $n_t$  transmitted signals, and  $y(t)$  is a vector  $n_r \times 1$  corresponds to the  $n_r$  received signals and  $u(t)$  is the additive white noise.

### 1.3 Need for Antennas

Since a spatial diversity system uses multiple antennas at the transmitter as well as at receiver, an antenna is the most important part of such systems. Transmitters and receivers require antennas in each and every case; some are inside laptop computers for Wi-Fi applications, or inside radio. Antenna is basically defined as the means of transmitting and receiving electromagnetic waves. It is the transitional structure between the free space and

the guiding space. [3] To couple electrical connection to the electromagnetic field antennas are required at radio receivers or transmitters which are used to carry signals/ information in the systems including Wi-Fi, broadcast radio, point to point communication links and many remote controlled devices[3].

### 1.3.1 Types of Antennas

Classification of Antennas is divided into different categories which are described below:

- **On the basis of radiation pattern**
  - i. **Omni-directional antenna:**

It radiates and receives in all directions also called as weakly directional antennas
  - ii. **Directional antenna:**

Another name is beam antennas as they radiate and receive in a particular direction.
- **On the basis of Aperture**
  - i. **Wire Antennas:**

These antennas are seen all around like on vehicles, buildings, ships aircrafts, space-crafts etc.
  - ii. **Aperture Antennas:**

These antennas majorly find applications in spacecraft and aircraft. Therefore these are more common to the layman today because of the rising need for more innovated form of antennas and also can be used for higher frequencies.
  - iii. **Microstrip Antennas:**

They consist of patch made of metal on grounded substrate and are low profile installed on the surface of aircrafts, space crafts, satellites, missiles.
  - iv. **Array Antennas:**

An aggregate of radiating elements called array gives radiation characteristics, better than single element antenna. The arrangement for arrays should be like that the radiations sum up to provide maximum radiation in a specific direction and minimum in other directions.
- **On the basis of polarization**

- i. **Linearly polarized antenna:** If an antenna transmits and receives in a vertical E direction then it is known as vertically polarized antenna. In the horizontal E direction antenna is transmitting/ receiving then it is horizontally polarized antenna.
- ii. **Circularly polarized antenna:** When antenna transmits/receives E field vectors of any orientation, then antenna is called as circularly polarized antenna.

The major requirement in the present wireless world is compactness of antenna, so from available structures for WLAN application; the microstrip antennas are the most optimum choice.

Since size and cost are important factors while implementing these antennas in RF devices, MSA are an optimum choice.

### 1.3.2 Introduction of Microstrip Patch Antenna

Another name of Microstrip antennas is patch antennas. Figure 1.6 shows a basic MSA geometry. The feed lines and the radiating elements are usually photoetched on the dielectric substrate. The shapes for radiating patch are such as squared, rectangular, thin strip (dipole), circular, elliptical, triangular, or any other configuration. The most common shapes are square, rectangular, dipole (strip), and circular because of ease of fabrication and analysis, and their attractive radiation patterns, especially low cross-polarization radiation. Small bandwidth and occupy less space are features of Microstrip dipoles, which makes them attractive for arrays. Using single elements or arrays of microstrip antennas, linear and circular polarizations can be achieved [3].

Microstrip element arrays with single or multiple feeds have better scanning capabilities and are able to achieve greater directivities. Numbers of substrates are used in the designing of microstrip antennas with their dielectric constants are in the range of  $2.2 \leq \epsilon_r \leq 12$ . For good performance by antenna thick substrates whose dielectric constant is in the lower end of the range are mostly in demand as they provide better efficiency, larger bandwidth, loosely bound fields for radiation into space, with the drawback of larger element size[3].

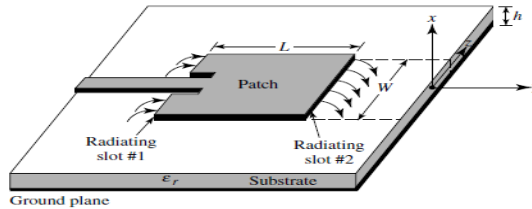


Figure 1.6 : Microstrip Patch Antenna [1]

### 1.3.3 Basic Characteristics of MSA Operation:

- i.) Designed in a way to have maximum pattern perpendicular to patch so that act as a broadside radiator. It is done by carefully selecting modes (field configuration).
- ii) As height of substrate increases, efficiency of antenna also increases which helps in increasing bandwidth. Surface waves are introduced due to increase in height of substrate, which degrades antenna pattern & polarization characteristics and can be eliminated by using cavity.
- iii) For rectangular patch, length of patch 'L' is  $\lambda_0/3 < L < \lambda_0/2$ . Dielectric sheet act as a separating element between ground plane and patch. There are many patch shapes, but we prefer dipole shaped patch as it requires lesser area, have large bandwidth[3].

### 1.3.4 Transmission line model

There are number of different models that are used for the Microstrip patch antenna analysis. These include transmission line model, full wave analysis & cavity model. Transmission-line model represents the microstrip antenna by two slots, which are then separated by a low-impedance  $Z_c$  transmission line of length L.

- **Fringing Effects**

Along the width and length of patch, dimensions of the patch are finite; therefore the field undergo fringing at the edges of the patch. Along the length it is shown in Figure 1.6 for the two radiating slots of the microstrip antenna. Also along the width the same applies. The amount of fringing depends on the height of the substrate and dimensions of the patch. For the principal E-plane fringing depends on the ratio of the patch length L to the substrate height h (L/h) and the dielectric constant of the substrate. Due to the fringing microstrip line looks wider electrically when compared with its physical dimensions. Because some of

the waves travel in the substrate and some in air, therefore an effective dielectric constant  $\epsilon_{eff}$  is introduced for fringing and the wave propagation in the line [3].

Values for the effective dielectric constant comes in the range of  $1 < \epsilon_{eff} < \epsilon_r$  for a line with air above the substrate and also depends on frequency. As the operational frequency increases, electric field lines mostly concentrate in the substrate. This is the reason microstrip line acts like a homogeneous line of one dielectric (only the substrate), and the effective dielectric constant gets closer to the value of the substrate's dielectric constant. The effective dielectric value of the substrate is given by:

$$\frac{W}{h} > 1 \tag{1.2}$$

$$\epsilon_{eff} = \frac{\epsilon_r + 1}{2} + \frac{\epsilon_r - 1}{2} \left[ 1 + 12 \frac{h}{W} \right]^{-1} \tag{1.3}$$

- **Effective Length & width and Resonant Frequency**

After getting affected by the fringing, patch's electrical length looks greater than its physical dimensions. Figure 1.7 presents the patch dimensions along its length which is elongated on each side by a length  $\Delta L$ , which is a function of the width-to height ratio ( $W/h$ ) and the effective dielectric constant. An approximate relation for the normalized extension is given by

$$\frac{\Delta L}{h} = 0.412 \frac{(\epsilon_{eff} + 0.3) \left( \frac{W}{h} + 0.264 \right)}{(\epsilon_{eff} - 0.258) \left( \frac{W}{h} + 0.8 \right)} \tag{1.4}$$

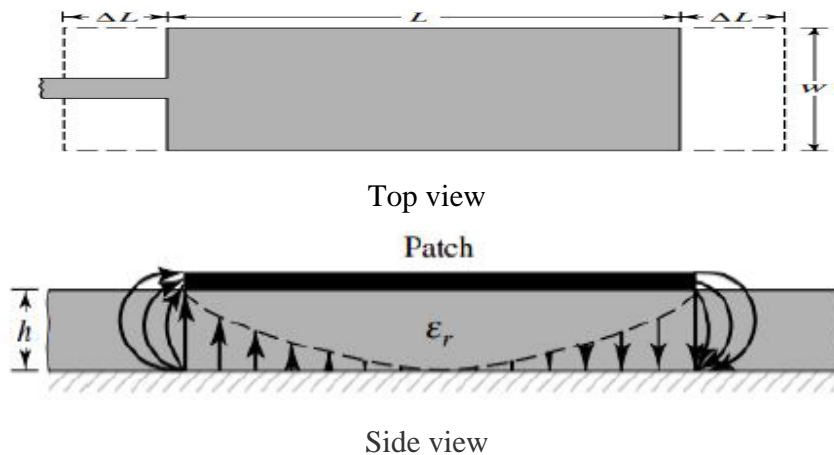


Figure 1.7 Physical and effective length of microstrip patch antenna

Due to effects of fringing patch's length has been elongated by  $\Delta L$  on each side, therefore the effective length of the patch is now given by

$$L_{eff} = L + 2\Delta L \quad (1.5)$$

For the dominant  $TM_{010}$  mode, the resonant frequency is given by

$$(fr)_{010} = \frac{1}{2L\sqrt{(\epsilon_r)\sqrt{(\epsilon_0\mu_0)}}} - \frac{v_0}{2L\sqrt{\epsilon_r}} \quad (1.6)$$

$v_0$  is the speed of the light in free space

### 1.3.5 Feeding Techniques

There are number of feeding methods available for Microstrip patch antennas. These can be broadly divided into two categories- contacting and non-contacting. In contacting method radiating patch is directly energized using a microstrip line as a connecting element. Electromagnetic field coupling is done for transferring power between the radiating patch & the microstrip line in the non-contacting scheme. The four main feeding techniques are the microstrip line, co axial probe, aperture coupling and proximity coupling [3].

#### 1.3.5.1 Microstrip line feeding

Microstrip line is one of the popular methods of feeding and easy to fabricate it has a conducting strip connected with the patch and review as patch's extension. Modelling is simple and easily matched by controlling the inset position. Drawback is increase in substrate thickness, surface wave and increase in feed radiation which bounds the bandwidth.

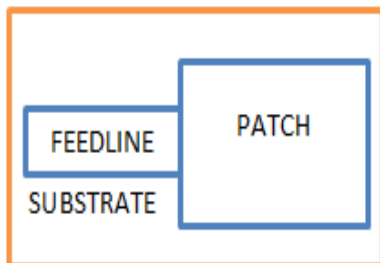


Figure1.8 (a) Microstrip Feeding

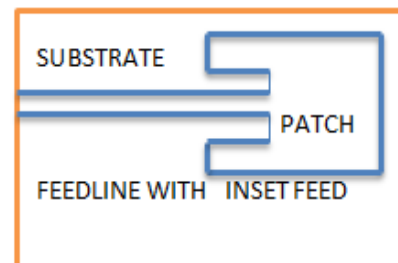


Figure1.8(b) Microstrip line with inset feed

#### 1.3.5.2 Coaxial Feeding

In this feeding an outer conductor of coaxial is connected to the ground plane while the inner conductor is connected to the patch of the antenna. It has several advantages such as simple to fabricate, matches easily and have low spurious radiations. Likewise disadvantages are narrow bandwidth, it is difficult to model especially for thick substrate and generates higher order modes which results in cross polarization.

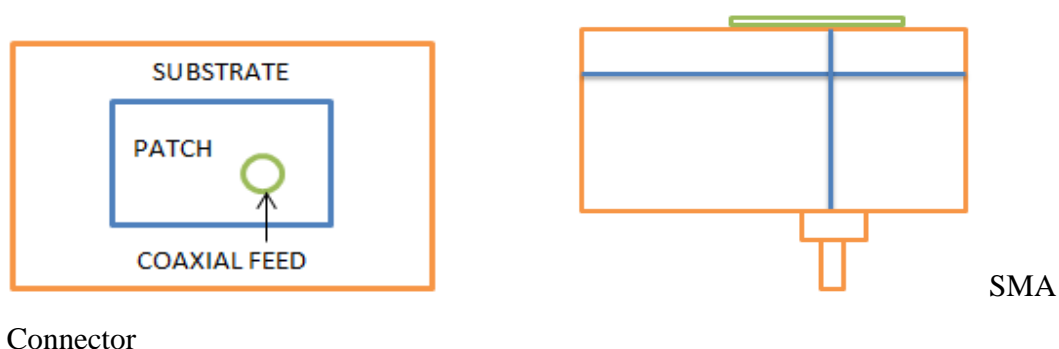


Figure 1.9 Co-axial Feeding

### 1.3.5.3 Aperture Coupling

This method comprises of two different substrates separated by a ground plane. On the lower side of lower substrate, microstrip feed line is present whose energy is integrated to the patch through a slot in the ground plane dividing two substrates. It allows unconventional optimization of the radiating element and the feed mechanism. Normally the bottom substrate uses a thin high dielectric constant substrate and top substrate uses a thick low dielectric constant substrate. The ground plane present in the middle of two substrates, insulates the feed from radiating element and reduces interference of spurious radiation for forming pattern and polarization purity[3].

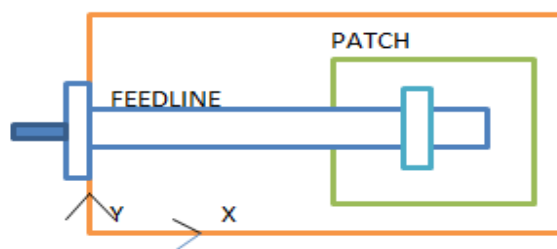


Figure 1.10 Aperture coupling

### 1.3.5.4 Proximity Coupling

Among all feeding techniques it has largest bandwidth and low invalid radiation, fabrication is quite difficult. Match is being controlled by using length of feeding stub and width-to-length ratio of patch.

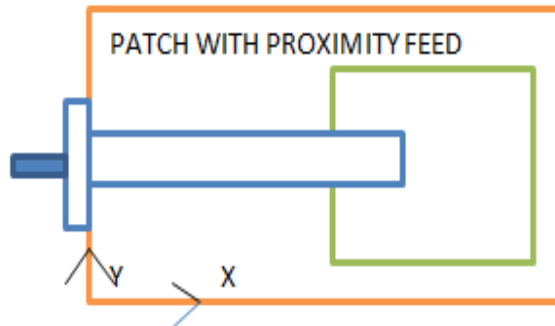


Figure 1.11 Proximity coupling

Since among all the feeding methods microstrip line feeding is the most simplest to implement and it more reliable with the easy impedance matching and more spurious feed radiations so it is better to implement the MSA with microstrip feeding.

### 1.4 Numerical Analysis of Microstrip Antennas

The numerical analysis for planar antennas is done by various theoretical techniques that are majorly used in electromagnetics. Full wave solvers is the Modeling technique which is introduced and categorized depends on their solution method: Finite Elements (FE) , Integral Equations (IE) solved by Method of Moments (MoM), Finite Differences in the Time Domain (FDTD), and Finite Integration Technique (FIT).

- **Integral equation techniques**

An integral equation technique uses maxwell's equations in form of integral equation to build the electromagnetic problem with respect to unknown currents flowing in the object.

- **Differential equation techniques**

To obtain differential equations from Maxwell's curl equations or the Helmholtz wave equations directly, we have the most popular Differential equation- based methods which are the Finite Element Method (FEM), and the Finite-Difference Time Domain method (FDTD), which is appointed by CST's Time Domain transient solver. CST Microwave Studio (CST MWS) is based on FDTD technique as it works by discretizing maxwell's integral equations and uses central differences for time derivatives.

### 1.4.1 Finite-Difference Time-Domain technique (FDTD)

The FDTD method is a time domain grid-based differential numerical modeling methods. For the application in electromagnetics, in FDTD method, the time-dependent Maxwell's equations (in partial differential form) are discretized by using central-difference approximations to the space and time partial derivatives. In the Maxwell's differential equations time derivative of the E-field is determined by the curl of the H-field, and the time derivative of the H-field is determined by the curl of the E-field. The final finite-difference equations are answered in a leapfrog manner.

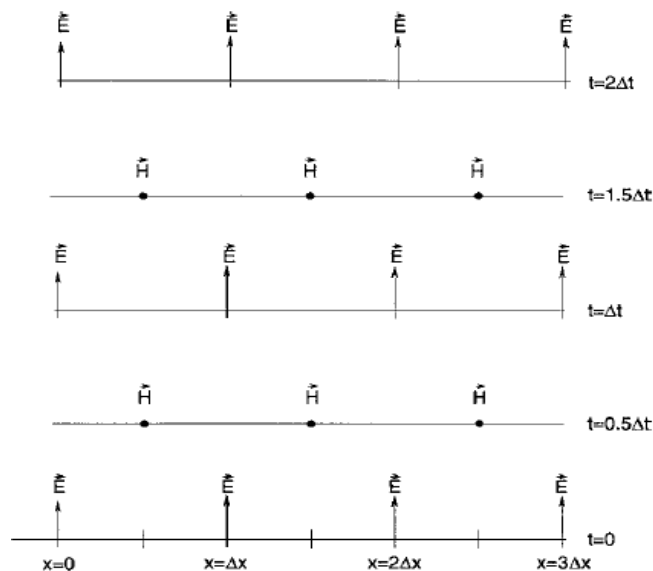


Figure 1.12 Leap frog algorithm used in the FDTD technique

In the leap frog algorithm E-field and H-field are shifted in space by half cell and in time by a half time step. E-field calculations are started from time  $t = 0$ , then after half time e.g.  $t = 0.5\Delta t$  H-field is calculated. This addition of half-time step continues alternatively in E and H-field. Similarly addition of half cell (e.g.  $0.5 \Delta x$ ) in space is done for E and H-field.

### 1.4.2 Theoretical Analysis of FDTD Method

The FDTD method comprises of discretization and result of Maxwell's curl equations in time domain given as:

$$\overrightarrow{\text{curl}}\vec{E} = -\mu \frac{\partial \vec{H}}{\partial t} \quad (1.7)$$

$$\overrightarrow{\text{curl}}\vec{H} = -\varepsilon \frac{\partial \vec{E}}{\partial t} + \vec{j} \quad (1.8)$$

The maxwell's equations are derived from 7 & 8

### 1.) Discretization Method

Scheme of discretization was first introduced by Yee [4] which contains Taylor development and first derivative is written as:

$$\frac{\partial f(x_0)}{\partial x} = \frac{f(x_0 + \frac{\Delta}{2}) - f(x_0 - \frac{\Delta}{2})}{\Delta} + \theta(\Delta^2) \quad (1.9)$$

$x_0$  Derivative calculation point

$\Delta$  Increment

The structure is decomposed into cubic elementary cells, also called Yee grid cells. In fig six components of electromagnetic field are determined. Discretization in time domain is carried out so that Electric and Magnetic field are interlaced.[4] Calculation of field is done by using FDTD at distinct locations and time on a grid. The fields are replaced as an indexed function using integers:

$$f(i\Delta x, j\Delta y, k\Delta z, n\Delta t) = f(i, j, k, n)$$

where  $\Delta x$ ,  $\Delta y$  and  $\Delta z$  are space increments

$\Delta t$  is the time increment.

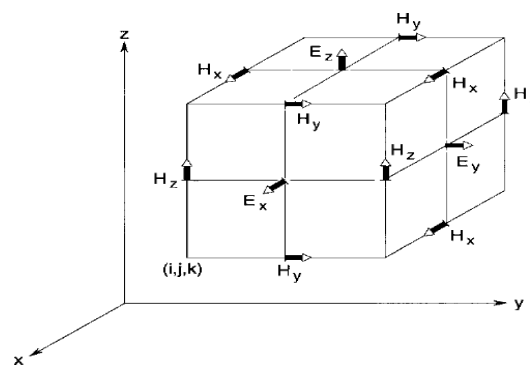


Figure 1.13 Field calculation points

Because central differences are used in equation (1.9) for derivatives, and the magnetic (electric) field is found from space derivative of electric(magnetic) field, the magnetic and electric field need to be spaced a half- space interval. The time derivative becomes

$$\frac{\partial f(i,j,k,n)}{\partial t} = \frac{f(i,j,k,n+\frac{1}{2}) - f(i,j,k,n-\frac{1}{2})}{\Delta t} \quad (1.10)$$

and it means that electric and magnetic components are scattered at  $\frac{\Delta t}{2}$  times that produce a leap frog algorithm. An example of  $E_x$  calculation is given by equation (1.10)

$$E_x^{n+\frac{1}{2}} = E_x^{n-\frac{1}{2}}(i,j,k) + \frac{\Delta t}{\epsilon} \left[ \left( H_z^n \left( i + \frac{1}{2}, j + \frac{1}{2}, k \right) - H_z^n \left( i + \frac{1}{2}, j - \frac{1}{2}, k \right) \right) / \Delta y - \left( H_y^n \left( i + \frac{1}{2}, j, k + \frac{1}{2} \right) - H_y^n \left( i + \frac{1}{2}, j, k - \frac{1}{2} \right) \right) / \Delta z \right] \quad (1.11)$$

Equation (1.11) is obtained after applying the leap frog algorithm to the E- field and H- field components.

### 1.4.3 FDTD Gridding Structure

In this gridding scheme, positions of electric and magnetic field are interchanged in a suitable fashion for the application of cavity model approach to antenna.

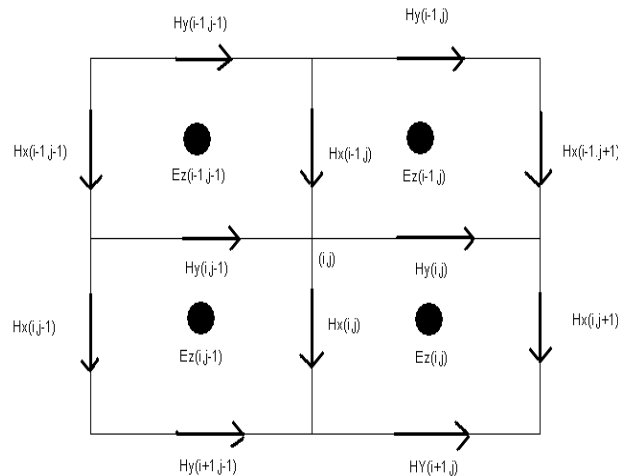


Figure 1.14. The new FDTD gridding scheme

The corresponding equations are:

$$\begin{aligned}
Ez^{n+1}(i,j) &= Ez^n(i,j) + \frac{\Delta t}{\varepsilon} + (Hy^{n+\frac{1}{2}}(i+1,j) - Hy^{n+\frac{1}{2}}(i,j))/\Delta x + (H \\
&\quad - Hx^{n+\frac{1}{2}}(i,j))/\Delta y \\
Hx^{n+\frac{1}{2}}(i,j) &= Hx^{n-\frac{1}{2}}(i,j) - \frac{\Delta t}{\mu} (Ez^n(i,j-1) - Ez^n(i,j))/\Delta y \\
Hy^{n+\frac{1}{2}}(i,j) &= Hy^{n-\frac{1}{2}}(i,j) - \frac{\Delta t}{\mu} (Ez^n(i,j) - Ez^n(i-1,j))/\Delta x
\end{aligned} \tag{1.12}$$

The new gridding scheme is presented to analyze any desired microstrip patch shapes. In this scheme, the positions of magnetic and electric fields are interchanged for the application of the cavity model approach to the antenna. A triangular antenna can be assumed as a cavity with perfect electric conductor (PEC) walls of triangular shape at the top and ground plane and by perfect magnetic conductor (PMC) walls on slots 1, 2 and 3. Along slots 1 and 2, the walls are implemented by setting  $H_x = 0$  and  $H_y = 0$  to zero. To implement slot 3 (PMC), wall is assumed to run such that it intersects the  $Ez$  components in the middle of the cells. The  $Ez$  components are updated by contour integral approach [4]. Considering the cell shown in Fig. 1.15, the  $Ez$  equation can be written as (the dotted line represents (PMC):

$$Ez^{n+1}(i,j) = Ez^n(i,j) + \frac{2\Delta t}{\varepsilon} + \frac{(Hy^{n+\frac{1}{2}}(i+1,j) - Hy^{n+\frac{1}{2}}(i,j))/\Delta x + (Hx^{n+\frac{1}{2}}(i,j) - Hx^{n+\frac{1}{2}}(i+1,j))/\Delta y}{2} \tag{1.13}$$

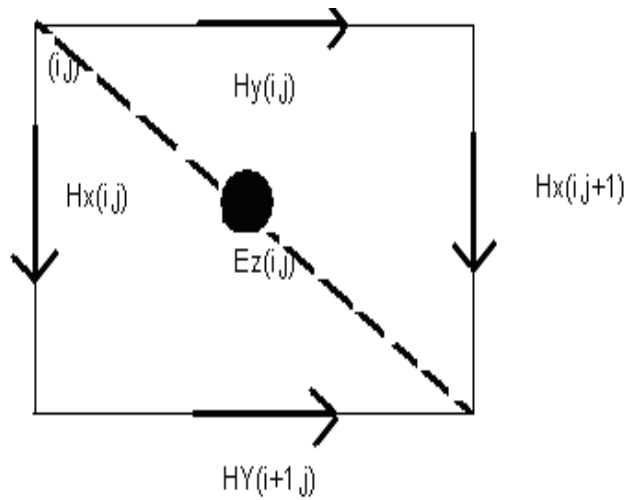


Figure 1.15 Intersection of PMC for slot 3 representing slanted edge of the antenna

Fig1.15 justifies the equation (1.13) which is obtained after reducing the 3D gridding structure of the FDTD cell to the 2D structure, using the cavity model approach. Using this approach a simple method for the FDTD analysis of Triangular shaped patch is developed.

### **1.5 Research Gaps**

An extensive literature review was carried out in the field of MSA and is presented in chapter 2, a lot of work is available regarding broadband antenna performance from MSA [] using DGS (Defected microstrip structure), fractals, slot shaped antennas but since not much work is reported regarding the use of MSA array in MIMO. In this thesis work antennas have been designed and tested for MIMO applications.

### **1.6 Objective of the thesis**

- Theoretical Analysis of a Triangular Patch Antenna.
- Designing and simulation of a single band slotted microstrip rectangular patch antenna and study of its various parameters.
- Designing and simulation results of single band slotted microstrip triangular patch antenna and study of its various parameters.
- Designing simulation and testing of results of a wideband fractal microstrip triangular patch antenna array for MIMO wireless applications.
- Designing simulation and testing results of a complementary microstrip triangular patch antenna array with defective ground structure using microstrip feed for MIMO wireless applications.

### **1.7 Thesis Organization**

The thesis is comprises of six chapters.

Chapter 1 includes introduction of wireless Communication and Microstrip antenna.

In Chapter 2 literature survey on the triangular patch microstrip antenna is presented which includes the researches done for bandwidth enhancement, defected ground structure and fractal antenna, correlation coefficient.

In Chapter 3, a single band microstrip antenna are designed, analyzed and studied.

Chapter 4, presents wide band triangular patch microstrip antennas design , simulation and analysis.

Chapter 5, includes the testing results of fabricated antenna studied in Chapter 4

In Chapter 6, conclusion and the future work is mentioned

## Chapter 2

### Literature Review

---

This chapter presents an extensive survey of work done in the field of Triangular Patch Microstrip Antenna; the literature survey is used as a ground work for designing antennas for MIMO applications for future.

#### 2.1 Microstrip Antennas

**R. G Vaughan** *et al.* [5] in 1987 investigated the conditions for antenna diversity; a condition is shown in which the incident and the far field of the diversity antenna follow relationship of orthogonality. According to him the responsibility of mutual coupling is principle, and distinct from that in a standard array antenna. A sufficient condition for diversity action for high gain antennas at the mobile is found , which approaches that most of mobile antennas, have zero (or low) mutual resistance between elements.

**A. Reineix** *et al.* [25] in 1989 studied microstrip patch antennas, using the finite difference time domain (FDTD) method in time domain. He made some alterations in the traditional FDTD method to review the microstrip antennas. Also he found that FDTD method allows a careful analysis of one or several dielectric interfaces using different excitation methods (coaxial, microstrip lines, etc.).

**C. Peixeiro** *et al.* [22] in 2011 presented an historical perspective of the development of microstrip antennas by analyzing the early years of microstrip antennas and examining the present situation of microstrip antenna field and trends of possible future evolution and the time period for analysis is divided into three stages: the early stage, the fast development period and the last decade.

**T. Gunasekaran** *et al.* [24] in 2013 focused on design of single microstrip patch antenna and linear array configurations by optimizing the various antenna parameters such as directivity, gain, Mutual coupling and beam width etc., designs and simulations were carried out using IE3D for WiMAX application at 2.4GHz operating frequency, it is

proposed that the linear array promises very narrow beam width with optimized gain in comparison to the optimized single patch with poor directivity and gain.

## **2.2 Microstrip feed antennas with different geometries**

**A.A. Rasheed** *et al.* [7] in 1994 experimented circular polarization (CP) with a single feed microstrip antennas. Circular polarization had been acquired using single feed-point from V-shape and trapezoidal microstrip antennas with an axial ratio bandwidth of 58 MHz and 50 MHz respectively. The benefit of these configurations was that their lesser area in contrast to other prevailing configurations with similar axial ratio bandwidth was achieved successfully.

**M. Zweeki** *et al.* [26] in 2001 investigated the broadband analysis of a microstrip patch antenna by using the Finite Difference Time Domain (FDTD) method. He discussed effects after changing the ground plane and dielectric size in opposition to the return loss at the input port and the far fields, addressed two distinct methods of antenna feeding and presented the problem of requirements for space size in the FDTD method. The frequency response of several patch antennas was discussed over wide bandwidths, using Gaussian pulses with a total bandwidth of 20GHz.

**L. H. Weng** *et al.* [18] in 2008 focused on the tutorial overview of defected ground structure (DGS) introduced the basic concepts and transmission characteristics of DGS and presented the equivalent circuit models of varieties of DGS units. Finally, after summarizing the main uses of DGS for field of microwave technology, the extension trend of DGS was given.

**A. Arya** *et al.* [35] in 2010 developed the defected ground structures (DGS) to improve characteristics of microwave devices, it has advantages in the area of the microwave filter design, microwave couplers to increase the coupling, microwave oscillators, microwave amplifiers, etc., also used in the microstrip antenna design for various applications such as antenna size reduction, cross polarization reduction, mutual coupling reduction in antenna arrays, harmonic suppression etc. which is motivated by a study of

Photonic/Electromagnetic Band gap structures, by etching of one or more PBG element defect in the ground plane was created.

**C.Poongodi** *et al.* [33] in 2011 presented the simulated capacity results when echelon, H-shaped, V -shaped free standing dipoles and printed dipole arrays were used in the MIMO systems. Different configurations have dipoles oriented in different directions; the channel model for multi-polarized antennas is used in the simulations. The performances of arrays are evaluated using capacity as the metric and mutual coupling was also considered between the dipoles of different orientations.

**Y. S. H. Khraisat** *et al.* [31] in 2012 demonstrated various shapes of microstrip array antennas, such as rectangular and triangular patch antennas array and designed 4x1, 2x1, and single element of both shapes and simulated them by a full wave simulator (IE3d) also presented a comparison between both rectangular and triangular antenna arrays.

**M. Bhardwaj** *et al.* [30] in 2014 discussed and analyzed the microstrip feeding method for rectangular patch antenna to discuss the result in terms of return loss, bandwidth, gain, directivity and current distribution using CST MWS 2010 for simulation.

**C.Y.D. Sim** *et al.* [39] in 2015 proposed a dual-band planar long term evolution (LTE) antenna design of size 40 mm × 15 mm × 0.8 mm, with reduced ground effects, so that the ground plane size can be altered without altering performance by antenna, this proposed antenna can be considered for laptop computer application for two-antenna multiple input multiple output (MIMO) system, and due to reduced ground effects and low envelope correlation coefficient (ECC) obtained in the results.

### **2.3 Triangular Patch Microstrip Antennas**

**N. Kumprasert** *et al.* [6] in 1994 used nearby solution of the capacitance of circular microstrip disk with the fringing fields for calculation of the resonant frequency formula for equilateral triangular patch microstrip antenna. The hypothetical results obtained were in good accordance with the innovatory data.

**R. R. Ramirez** *et al.* [8] in 2002 analysed equilateral triangular patch microstrip antennas for the calculation of mutual coupling with the limitation of small spaces between elements. He designed four element diversity antennas that have capabilities of dual band and dual linear polarization. In this paper analysis of triangular microstrip antennas is given to find out the best placement for the reduction of the mutual coupling and total surface area. The best possible location was found near the midpoint along the edge of the antenna so that design is suited for dual mode 802.11a,b WAN levels.

**J.S. Kuo** *et al.* [10] in 2003 analysed a novel circular polarization (CP) design of a single-feed equilateral triangular microstrip antenna with enhanced antenna gain. He obtained the design by situating three triangular slots carefully at positions below the equilateral-triangular radiating patch in the ground plane. By modifying length of one of the triangular slot's side slightly greater than that of the others and making two orthogonal near-degenerate resonant modes to excite. Measured antenna gain was increased by 3.3 dBi in contrast to the same antenna height, substrate material, operational frequency and shape of radiating patch of equilateral-triangular microstrip antenna without triangular slots in the ground plane

**R. K Vishwakarma** *et al.* [11] in 2006 conducted experimental investigations on the equilateral triangular microstrip antenna to study the radiation pattern of two layer triangular patch antenna and found that two layer triangular patch radiate with maximum power , VSWR, return loss, etc.

**J.S. Row** *et al.* [12] in 2006 designed a short-circuited triangular patch antenna to operate it as a broadband by situating two walls shorted on the opposite edges of a tip-truncated V- shaped slotted triangular patch antenna with two resonant modes made to get excited at the same time & coupled together for broadband operation. Designing of an antenna prototype for covering UMTS and ISM bands (1.92–2.48 GHz) was completed and tested which give radiation patterns conical in nature and therefore, can be used for the wireless applications.

**F. Y. Zulkifli** *et al.* [14] in 2007 implemented defected ground structure (DGS) on linear array of triangular patch microstrip antennas to enhance the design and suppress surface waves. He experimentally found that the radiation performance of the antenna is due to DGS dimension by locating the DGS at particular position and measured results obtained for antenna with DGS shows improvement in impedance matching with good return loss and suppress cross polarization.

**F. Y. Zulkifli** *et al.* [19] in 2008 presented two element microstrip antenna array of triangular shaped patches with hexagonal shaped defected ground structure (DGS) implemented on the effect of varying geometry and dimension of the DGS on the radiation pattern of the antenna was observed. Simulation and measurement results ensured that the antenna with DGS had better characteristics than the antenna without DGS. Antenna with hexagonal DGS had enhanced axial ratio bandwidth and radiation properties of the antenna than the antenna without DGS.

**A. Deb** *et al.* [27] in 2010 proposed a novel finite difference time domain (FDTD) scheme for the analysis of triangular microstrip patch antenna's characteristics, combined with the cavity model approach to reduce the entire problem to two dimensions to get fast and easy computation of the impedance and radiation characteristics of the antenna.

**J. Malik** *et al.* [38] in 2013 proposed a complementary sierpinski gasket fractal antenna of equilateral triangular shape resonator with proximity-fed in multilayer structure to obtain the dual-band behaviour for the applications of WiMAX and WLAN and designed an electromagnetic coupled stacked structure for dual-band wireless applications with two different patches operating at two frequencies (3.5 GHz WiMAX and 5.8 GHz wireless LAN).

**A. Kaur** *et al.* [43] in 2015 proposed design of aperture coupled stacked gasket fractal antenna for UWB (Ultra-wide band) and WLAN applications with the DGS structure in it. Layers of fractal patch were formed on the layers of FR4 substrate placed one above the

another to achieve wide bandwidth and circular polarisation. The proposed antenna gives dual band of bandwidth 630MHz (4.75-5.38GHz) and 400MHz (6.8-7.2GHz).

**S. Gupta** *et al.* [41] in 2015 proposed a Finite Difference Time Domain scheme for the analyzing triangular microstrip patch antennas by using coupled maxwell's curl equations in the time domain. A cavity model approach was used to reduce the entire problem to two dimensions which resulted in fast and easy computation of impedance and radiation characteristics of antenna.

**S. Gupta** *et al.* [42] in 2016 proposed a microstrip fed fractal antenna array of two antennas (with equilateral triangle shapes on the triangular patch) to achieve the good bandwidth in the frequency range between 5.45 – 5.72 GHz for the wireless applications (WLAN band). Simulation results for this proposed antenna are presented in terms of bandwidth, gain and S parameters, which indicates the desired performance of antenna for wireless applications .The antenna array has been propose for MIMO applications and the capacity calculations for an ideal MIMO environment of a system with 1 x 2 diversity were also presented.

## 2.4 MIMO Antenna Arrays

**S. Blanch** *et al.* [9] in 2003 designed antennas for MIMO systems and described a simple formula to calculate the envelope correlation of an antenna diversity system from the S-parameter of the antenna system which also gives the advantage of understanding the mutual coupling consequences and input meeting the diversity performance of the antenna system. To grow spectrum efficiency of wireless systems antenna diversity was acknowledged. He also discovered that mutual coupling of the antenna deteriorates the performance of a diversity antenna system.

In context to the increase in channel capacity because of MIMO systems,

**A. Goldsmith** *et al.* [2] in 2003 gave summary of the results for the Shannon capacity of single-user and multiuser multiple-input multiple-output (MIMO) channels. After providing abstract for the results of ergodic and capacity versus outage for single-user MIMO channels, the results obtained shows that the increase in capacity received from

multiple antennas based on the channel information available at receiver or transmitter, signal-to-noise ratio of channel, and the correlation between the channel gains of each antenna present. He found the relation where capacity region of the MIMO multiple access and the largest known achievable rate region for the MIMO broadcast channel were related by duality transformation which helped in detecting the transmission strategies to achieve a point on the boundary of the MIMO MAC capacity region. Finally, capacity results of multi cell MIMO channels with base station cooperation were discussed.

**B. Clerckx** *et al.* [13] in 2007 analysed the effect of mutual coupling generated by two closely spaced antennas with minimum scattering at the subscriber unit on  $2 \times 2$  multiple-input multiple-output channels also, considering impact of (de)correlation and antenna gain variation due to coupling technique and highlighting the work of inter element spacing, the richness of scattering and the array orientation which gives useful understanding of mutual coupling effect on system capacity and performance.

**S.Ranvier** *et al.* [15] in 2007 presented a technique to increase both mutual coupling and efficiency which was based on hardware modification and removes the drawback of mutual coupling over a certain frequency band, also it enhances the amount of energy moved from one radiating element to the other and the amount of energy is reduced at the port of the coupled antenna.

**C.A. Tunc** *et al.* [16] in 2008 experimented and simulated the printed dipole arrays performance in the MIMO channel with the help of channel model using electric-field integral equation and explored the impacts of the electrical properties (such as the dielectric thickness and permittivity) on the MIMO capacity. Also, presented the several dielectric-substrate configurations contributing high-capacity MIMO arrays.

**H. Zhang** *et al.* [17] in 2008 presented 2.65 GHz MIMO antenna design with three equilateral triangular microstrip patches and found their wide-beam characteristics combined with each antenna element of the high gain, SNR improvement and interference

rejection of the MIMO system by analysing correlation and mutual coupling between antenna ports pairs.

**A. Ocalanet et al.** [20] in 2009 designed and analysed a uniform linear antenna array of compact space-multimode stacked circular microstrip patch for MIMO-OFDM WLAN systems and compared the associated spatial and modal correlation, ergodic spectral efficiency and compactness gains with dipole and circular microstrip patch uniform linear arrays.

**D. Shen et al.** [32] in 2010 analytically investigated the capacity of wireless channels in multiple input multiple output (MIMO) system over different types of wireless fading channels, such as Rayleigh, Rician and Nakagami fading channels. Firstly investigated and analytically derived the channel capacity of the Rayleigh-Lognormal fading channel in integral form. It gave the Eigenvalue Probability Density Function (PDF) of the lognormal fading channel using two numerical calculation methods; Gaussian-Hermite numerical integration, and Gaussian-Laguerre numerical integration.

**C. A. Tunc et al.** [21] in 2010 analyzed and measured the performance of printed rectangular patch antennas array using a full-wave channel model in an indoor environment, and explored the effects of mutual coupling and the electrical properties such as thickness of the dielectric material and relative permittivity and on the MIMO capacity.

**C. Votis et al.** [36] in 2010 investigated the importance of envelope correlation coefficient “ $\rho$ ” on propagation paths of the different RF signals in a  $2 \times 2$  MIMO antenna array system and approached the value for this coefficient which is evolved from a simple closed-form equation varies from 0 to 1. Also, different configurations for antenna array show that the calculated “ $\rho$ ” has very small values and approaches to zero which shows quite perfect action and performance of MIMO system.

**L. Hanlen et al.** [1] in 2012 gave expressions for the capacity of multiple-input multiple-output channels with the channel gains have a correlated complex normal distribution and

receivers with independent Gaussian noise and signalize the input density via a necessary and sufficient condition for optimality. The resulting capacity depend on the channel correlation matrices and expressed in terms of hypergeometric functions of matrix argument.

**F. Y. Zulkifli** *et al.* [4] in 2013 proposed a compact slot ring triangular patch antenna with stub designed for MIMO 2x2 broadband application, it consists of only one layer substrate; has broadband characteristic due to the slot ring inserted to the triangular patch antenna. He achieved mutual coupling suppression in MIMO 2x2 elements to lower than 25 dB by placing the single element perpendicular to each other.

**H. Li** *et al.* [23] in 2013 analysed the correlation coefficient of received signals across a pair of antennas for multiple-input–multiple-output (MIMO) systems and calculated the signal correlation between two antennas from their 3-D radiation patterns. The method is used to simplify measurement and reduce cost, especially for mobile handset MIMO antennas, it is based on the equivalent circuits of antenna arrays and achieved better accuracy for dipole antenna arrays and patch antenna arrays.

**S. Gupta** *et al.* [40] in 2015 presented a review article on the design of MIMO systems with three equilateral triangular patches and analysed the impact of mutual coupling on system performance, studied the wide beam characteristics and the high gain of each antenna element, SNR improvement and interference rejection for MIMO system considering both correlation effects and variation of antenna gain due to mutual coupling mechanism.

Based on the literature survey carried out, the objective of the thesis work is defined in chapter 1. These are taken up one by one in the subsequent chapters to present the research work carried out in this regard.

## Chapter 3

### Single Band Microstrip Antenna Design for WLAN Applications

---

In order to illustrate the basic concepts studied about design & fabrication of microstrip antennas. In this chapter, the design of single band microstrip antenna using microstrip line feeding is proposed for WLAN applications. The antenna design is done using transmission line model equation mentioned in chapter 2. Another triangular single band MSA is designed to resonate at GHz for WLAN application to illustrate the usage of basic MSA concepts. The design is carried out using CST MWS V'10.

#### 3.1 Design of Single Band Slotted Rectangular Patch Microstrip Antenna at 5.2GHz

A single band slotted rectangular patch antenna is designed for resonant frequency of 5.138 GHz using transmission line model [6]. In this section the design of rectangular microstrip patch antenna is explained satisfying the given specifications.

Table 3.1 Design Specifications of Single Band Antenna

Frequency ( $f_r$ )	5.138
Dielectric Constant ( $\epsilon_r$ )	4.4
Patch Substrate Thickness	1.57mm
Feed Substrate Thickness	1.57mm

Table 3.2 Optimized Dimensions of the Single Band Antenna

Parameters	$L_p$	$W_p$	$L_g$	$W_g$	$L_f$	$W_f$
Description	Length of Patch	Width of Patch	Length of Ground	Width of Ground	Length of Feedline	Width of Feedline
Values	26mm	11.8mm	32mm	28mm	14mm	3.2mm

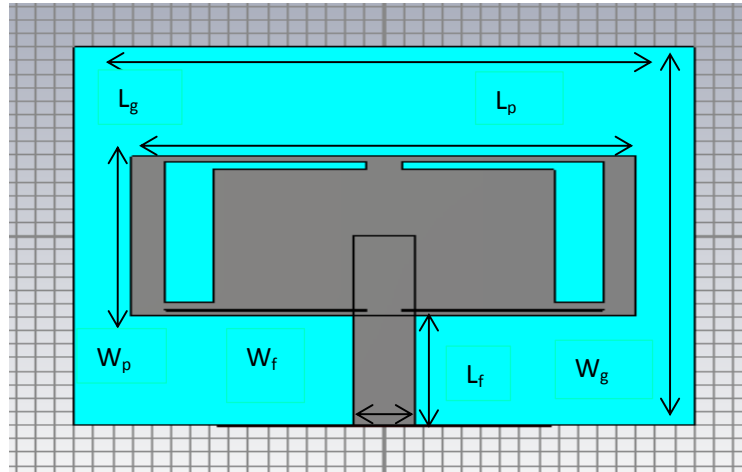


Figure 3.1 Geometry of proposed U-slot Rectangular Patch Antenna on CST Studio

### 3.1.1 Simulation Setup and Results

The antenna designing is carried out using CST MWS (Computer Simulation Technology Microwave Studio) 2010. CST MWS is a tool for the 3D EM simulation of high frequency devices such as antennas, couplers, planar and multilayer structures. It is exceptionally user friendly and enables the fast and accurate analysis. Figure 3.1 shows the front view of the antenna. The simulated results of the proposed antenna are presented in the below figures:

#### 3.1.1.1 Return Loss and Antenna Bandwidth:

Figure 3.2 shows the S-parameter as a function of frequency. The antenna resonates at 5.138 GHz with  $S_{11}$  parameter (return loss) value of  $-19.27\text{dB}$ . For this particular design the measured  $-10\text{ dB}$  bandwidth is 141 MHz. The higher value of the return loss indicates better coupling which in turn leads to higher value of the directivity and gain for the proposed antenna.

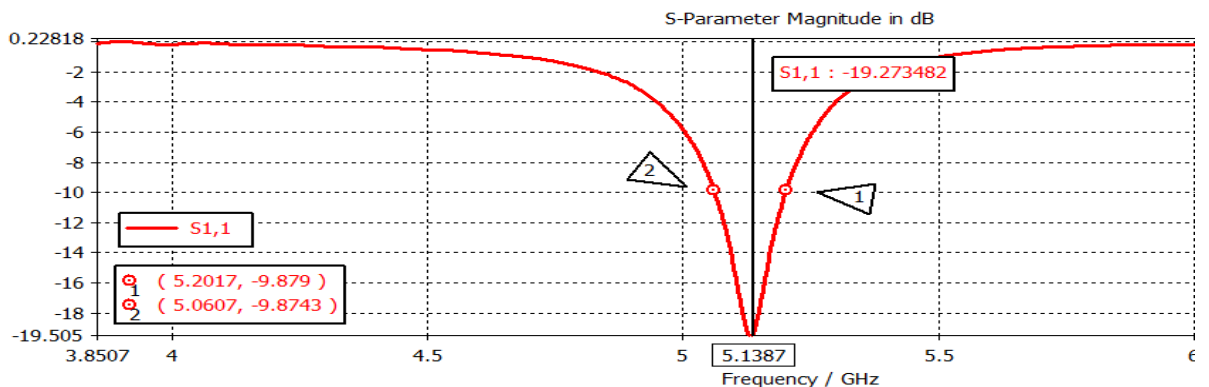


Figure 3.2 Return Loss  $S_{11}$  (in dB) of Simulated Antenna at 5.138GHz

### 3.1.1.2 Smith Chart and Antenna Impedance

Figure 3.3 shows the smith chart of the proposed single band antenna. It depicts the variation of antenna impedance with frequency. The size of the locus of the smith chart is controlled by the slot length and it increases with increase in the slot length. The locus must be large enough to pass the center of the smith chart for properly matched antenna.

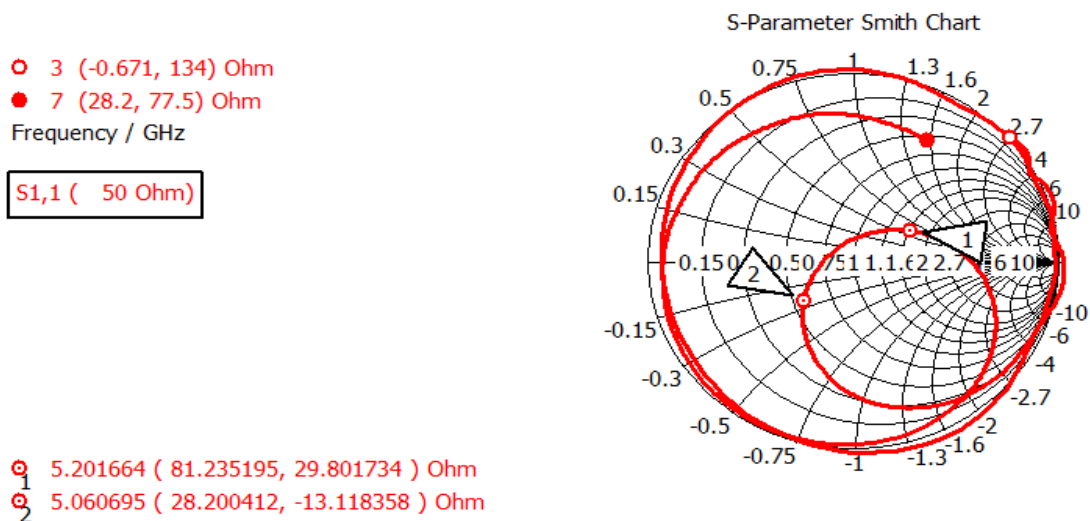


Figure 3.3 Smith Chart showing the Characteristics Impedance of the Single Band Antenna

### 3.1.1.3 Directivity

Figure 3.4 shows the 3D directivity plot of the antenna. It represents the antenna resonating at 5.138 GHz provides a directivity value of 6.401 dBi which means the designed antenna radiates more by an amount of 6.401 dBi in a particular direction when compared with an isotropic antenna which radiates equally in all directions. The magnitude of the main lobe is 6.4 dBi.

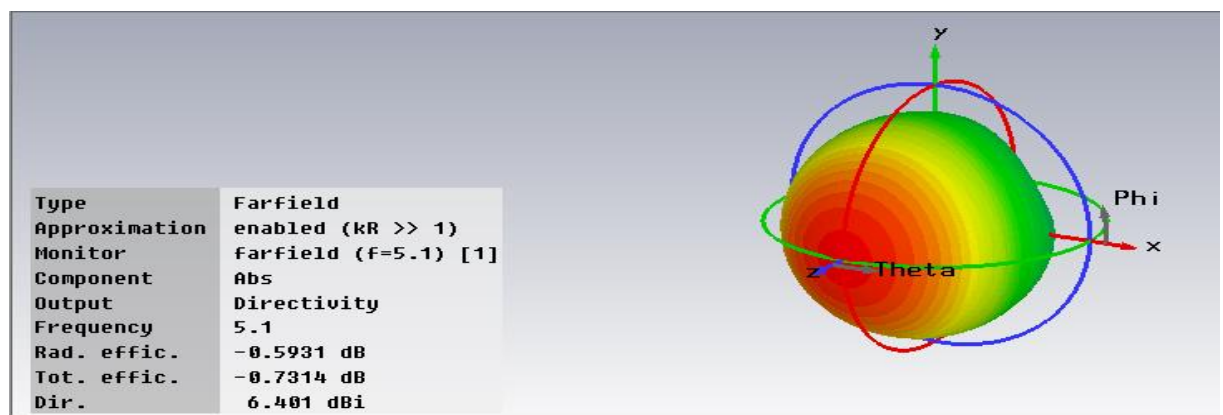


Figure 3.4 3D Radiation Pattern of the Directivity of the Single Band Antenna at 5.1 GHz

### 3.1.1.4 Current Distribution at resonant frequency of operation:

According to the current distributions, the slots of different dimensions were cut in the patch so as to get single band antenna for WLAN applications. Figure 3.5 shows that surface current at 5.138 GHz is highest near bottom of slot 1 and 2 proving that both slots are responsible for resonating at lower frequency band i.e. covering band from 5.06GHz to 5.20GHz. The maximum value of surface current is 87.6609A/m.

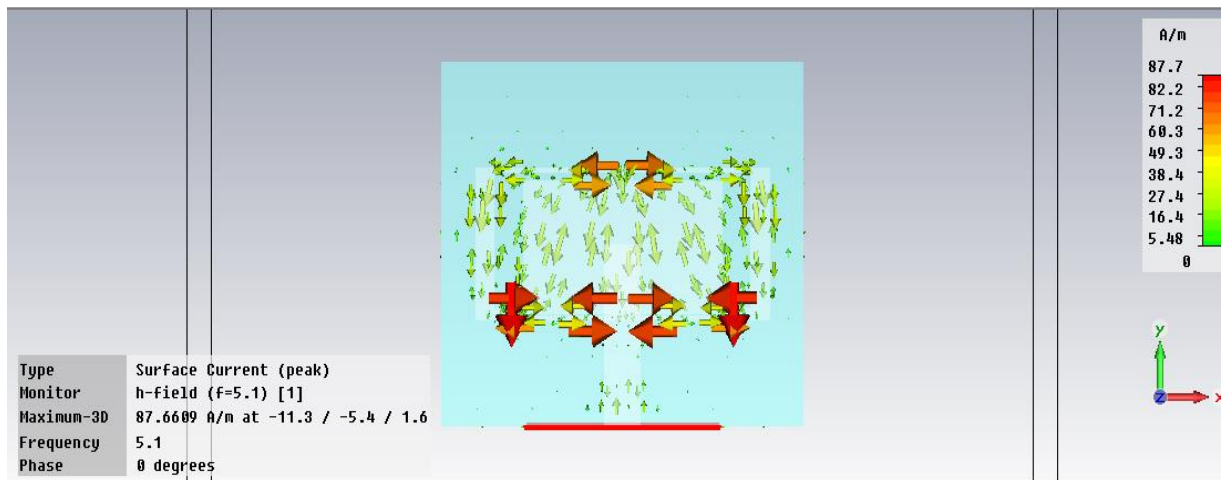


Figure 3.5 Current distributions at frequency 5.1GHz

Next subsection presents the design of a Triangular MSA for WLAN applications. A triangular antenna occupies lesser space as compared to a rectangular antenna so it is a preferred geometry for most of wireless applications.

### 3.2 Design of Single Band Slotted Triangular Patch Microstrip Antenna at 4.8GHz

A single band triangular shape microstrip patch with microstrip feeding is designed at frequency of 4.83 GHz for WLAN applications. The triangular patch is designed using design equation no. (3.1).

$$f = \frac{2c}{3a(\epsilon_r)^{\frac{1}{2}}} (m^2 + mn + n^2)^{1/2} \quad (3.1)$$

Where  $f$  = resonant frequency of triangular patch,  $c$  is velocity of light,  $\epsilon_r$  = dielectric constant and  $m, n$  are integers. In this section the dimensions of the ground plane and the substrates are calculated using transmission line model. The various design specifications of the proposed antenna are mentioned in Table 3.3.

Table 3.3 Design Specifications of Single Band Antenna

Frequency ( $f_r$ )	4.8GHz
Dielectric Constant ( $\epsilon_r$ )	4.4
Patch Substrate Thickness	1.57mm
Feed Substrate Thickness	1.57mm

Figure 3.6 shows the front view of designed antenna in CST MWS V'10. These parts are labelled and their values are mentioned in table 3.4

Table 3.4 Optimized Dimensions of the Slotted Triangular Patch Antenna

Parameters	$s$	$L_g$	$W_g$	$L_f$	$W_f$
Description	Side of Patch	Length of Ground	Width of Ground	Length of Feedline	Width of Feedline
Values	39.72 mm	68mm	68 mm	17 mm	1 mm

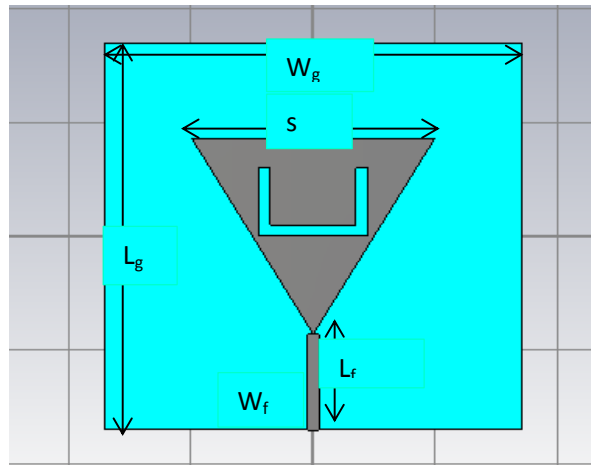


Figure 3.6 Geometry of proposed Antenna Design on CST Microwave Studio

### 3.2.1 Simulation Setup and Result of Triangular Patch Antenna

The simulated results of the proposed antenna are presented in the below figures:

#### 3.2.1.1 Return Loss and Antenna Bandwidth

Figure 3.7 shows the S-parameter as a function of frequency. The antenna resonated at 4.838 GHz with  $S_{11}$  parameter (return loss) value of  $-25.548$  dB. For this particular design

the measured  $-10$  dB bandwidth is 169 MHz. The higher value of the return loss indicates better coupling which leads to higher value of the directivity and more gain for the antenna designed.

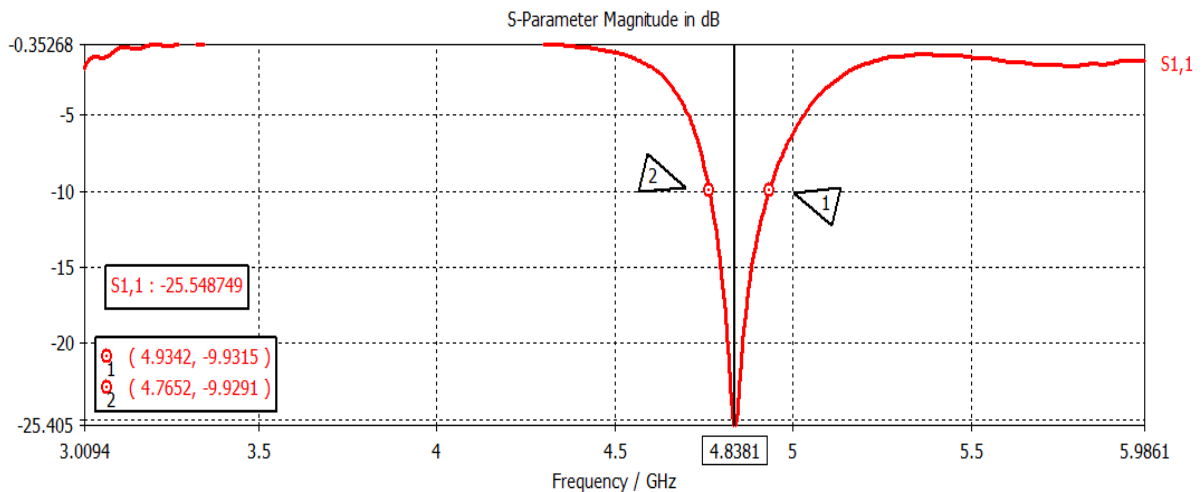


Figure 3.7 Return Loss  $S_{11}$  (in dB) of Simulated Antenna at 4.8GHz

### 3.2.1.2 Smith Chart and Antenna Impedance

Figure 3.8 shows the smith chart of the proposed single band antenna. The Smith Chart plot (figure 3.8) represents that how the antenna impedance varies with frequency. The size of the locus of the smith chart is controlled by the slot length and it increases with increasing the slot length.

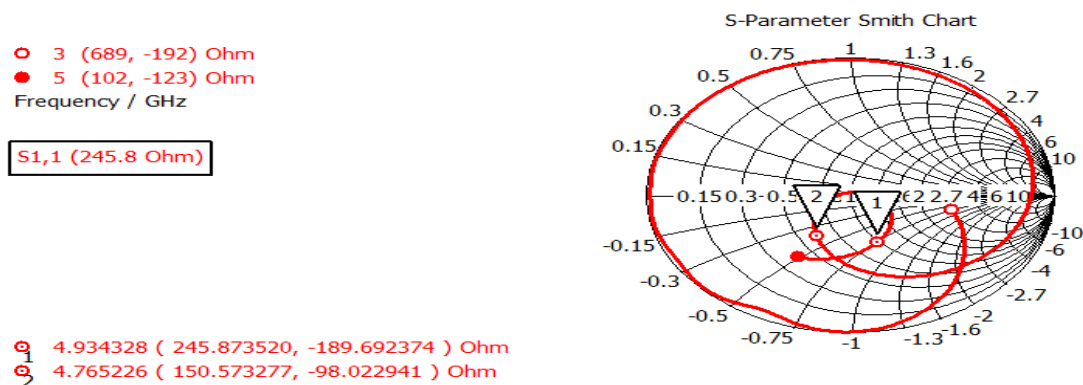


Figure 3.8 Smith Chart at 4.8GHz

### 3.2.1.3 Directivity

Figure 3.9 shows the 3D directivity plot of the antenna. It represents the antenna resonating at 4.83 GHz provides a directivity value of 6.583 dBi which means the designed

antenna radiates more by an amount of 6.583 dBi in a particular direction when compared with an isotropic antenna.

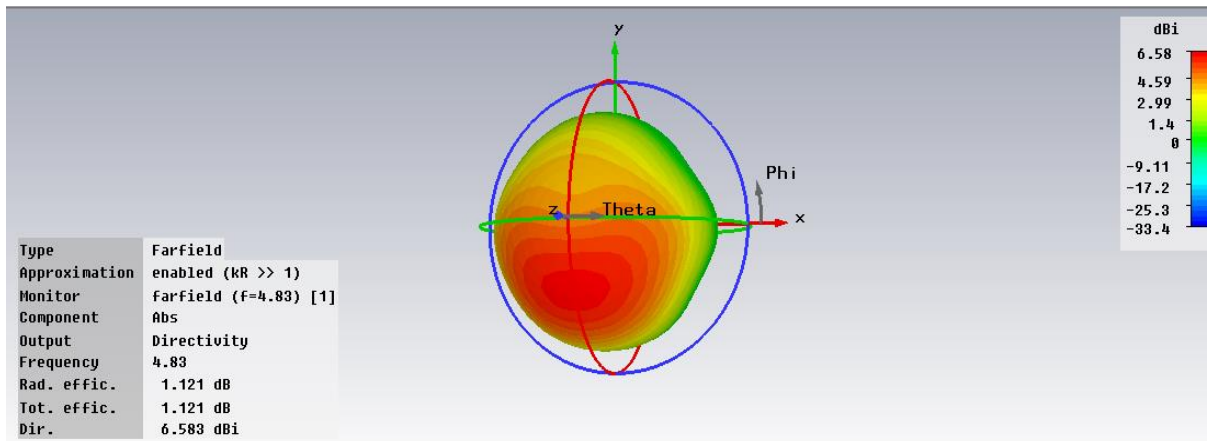


Figure 3.9 3D Directivity of slotted Triangular Patch Antenna at 4.8 GHz

### 3.2.1.4 Current Distribution at resonant frequency of operation:

According to the current distributions, the slots of different dimensions were cut in the patch so as to get single band antenna for WLAN applications. Figure 3.10 shows that surface current at 4.838 GHz is highest at the top of slot proving that this slot is responsible for resonating at frequency band i.e. covering band from 4.7652 GHz to 4.9342GHz. The maximum value of surface current is 54.3646A/m.

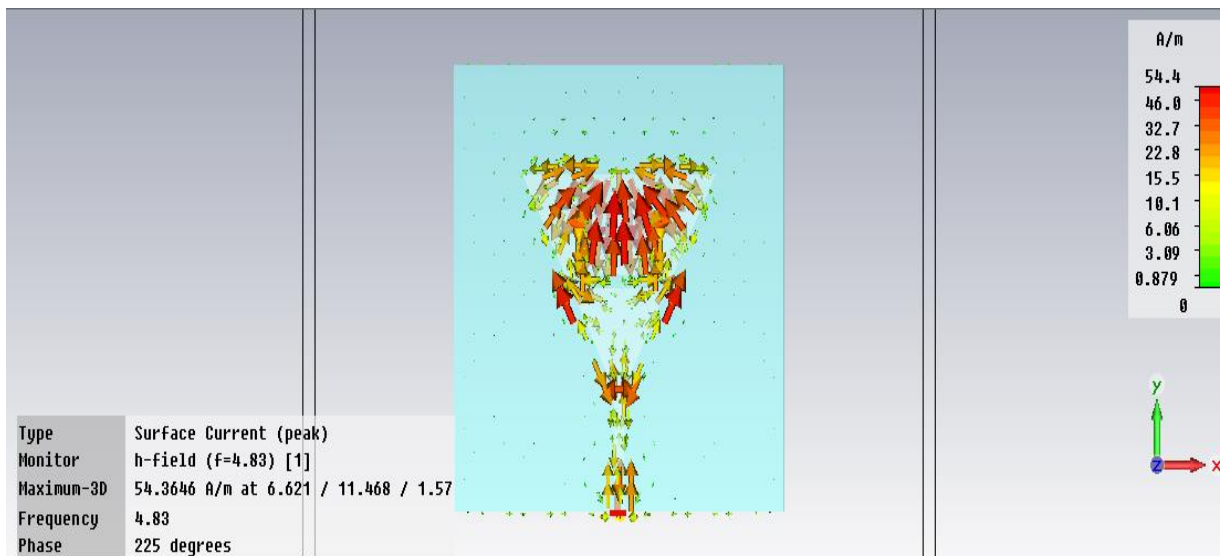


Figure 3.10 Current distributions at frequency 4.83 GHz

**Conclusion:**

This chapter presents the design of two single band MSAs for WLAN applications. The first design is regarding a rectangular MSA & the second design is regarding a triangular MSA as triangular pattern gives a higher bandwidth and a smaller size as compared to a rectangular patch antenna with microstrip feed. The antenna shows a gain of 6.401dBi and 6.583dBi respectively for WLAN application.

## Chapter 4

### Wide Band Microstrip Patch Antenna Arrays for MIMO in WLAN Applications

Need of increased capacity and bandwidth arises in wireless communication systems due to the significant advancement in wireless technology. To achieve these requirements MIMO systems was implemented. Channel capacity and minimum BER are the major requirements of MIMO systems which can be achieved using antenna arrays. In this section triangular patch antenna arrays were designed to realize MIMO system as they required low antenna height which solved the purpose of design compactness. This chapter presents the design of a complementary array for MIMO applications in WLAN systems.

#### 4.1 Design of Complementary Sierpinski Gasket Fractal Antenna Array for MIMO Applications with Defected Ground Structure:

A triangular complementary antenna array is designed in this section. The array has two triangular antennas with fractal geometry. Complementary triangles are attached on its face to get a dual band behavior. A slot is cut in its structure to further enhance its bandwidth. The antenna is designed on a FR4 substrate with microstrip feeding technique. Figure 4.1 shows the structure of this antenna and table 4.1 shows the design specifications followed while designing the antenna. The antenna was designed using equation no. 14 and the detailed parameter values are mentioned in table 4.2

Table 4.1 Design Specifications of Single Band Antenna

Frequency ( $f_r$ )	4.83GHz
Dielectric Constant ( $\epsilon_r$ )	4.4
Patch Substrate Thickness	1.57mm
Feed Substrate Thickness	1.57mm

Table 4.2 Optimized Dimensions of the Complementary gasket fractal Antenna

Parameters	s	$Lg$	$Wg$	$Lf$	$Wf$	$Ld$	$Wd$
Description	Patch side	Length of Ground	Width of Ground	Length of Feedline	Width of Feedline	Length of DGS	Width of DGS

Values	39.726 mm	128mm	128 mm	61.79mm	2mm	80mm	
--------	-----------	-------	--------	---------	-----	------	--

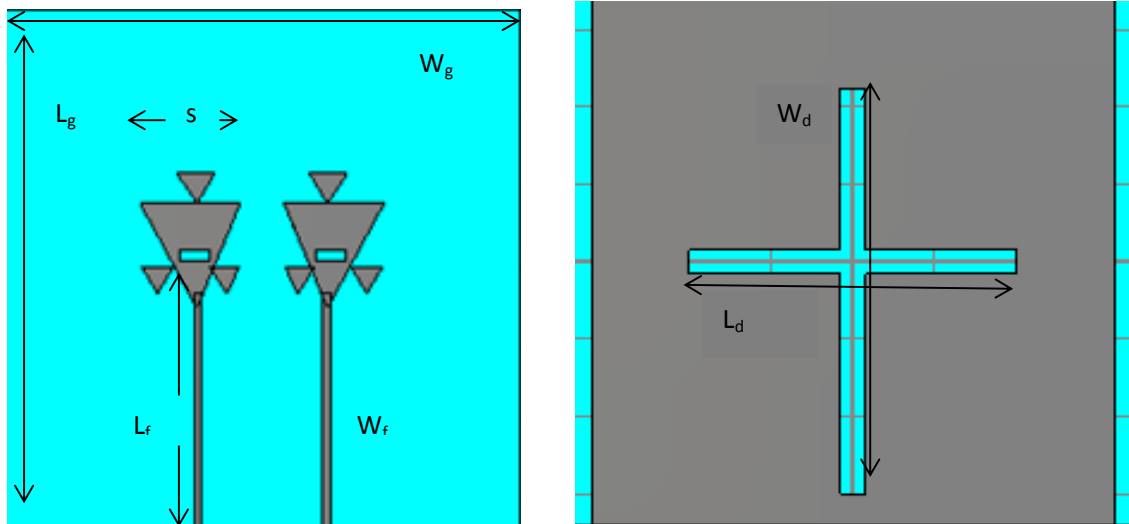


Figure 4.1 (a) Front view of proposed Antenna (b) back view of proposed antenna designed on CST microwave studio

#### 4.1.1 Simulation Setup and Result of Antenna

Designs and simulations of proposed antenna is done using CST MWS V'10 which is based on finite integration technique (FIT). The simulated results of the proposed antenna are present in the below figures.

##### 4.1.1.1 Return loss and Antenna Bandwidth

Return loss [ $S_{11}$  in dB] plot of complementary triangular patch antenna array is shown in figure 4.2. The antenna shows a peak return loss of is  $-36.059$ dB at resonant frequency at  $4.83$ GHz and bandwidth obtained is  $8.2\%$ . The  $-10$ dB bandwidth of antenna is  $408.2$  MHz from  $4.7 - 5.1$  GHz which makes the antenna suitable for WLAN applications. The higher value of the return loss indicates better coupling which leads to higher value of the directivity and more gain for the antenna designed. Figure 4.2 shows the parameter plot of the antenna with  $S_{11}$ ,  $S_{12}$  &  $S_{22}$ . Plot of  $S_{11}$  with respect to frequency shows that the antenna is resonant at frequency of  $4.83$  GHz and bandwidth of  $408.2$  MHz.

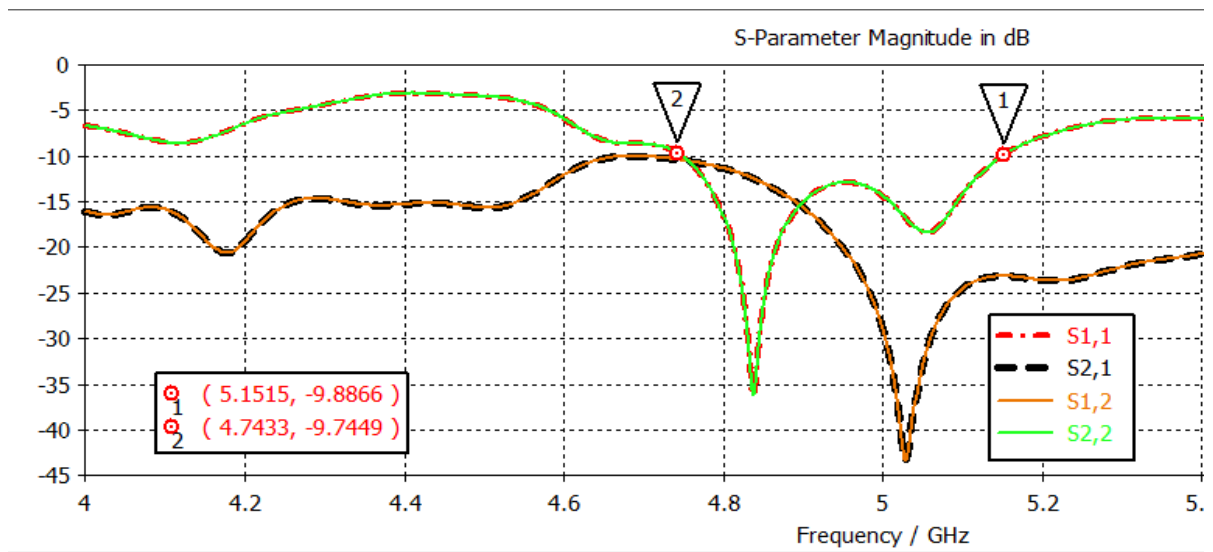


Figure 4.2 Return Loss  $S_{11}$  (in dB) of Simulated Antenna at 4.83GHz

#### 4.1.1.2 Smith Chart and Antenna Impedance

Loops in smith chart shows where the antenna and feed structure resonates and nearer the loop to the centre of the chart, better the impedance match. Smith chart for the proposed antenna is shown in the figure 4.3. It shows that antenna is matched to an impedance of 50ohms at two resonant frequencies.

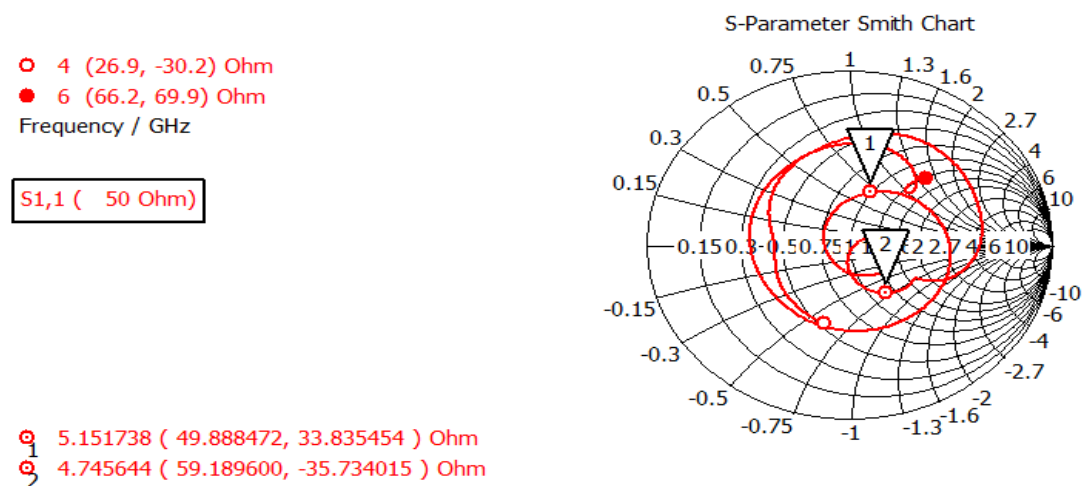


Figure 4.3 Smith Chart at 4.8GHz

#### 4.1.1.3 Directivity

Figure 4.4 shows the 3D directivity plot of the antenna. It represents the antenna resonating at 4.83 GHz provides a directivity value of 5.839 dBi when the excitation is

given to port 1 and same value of directivity e.g. 5.839dBi when excitation is given to port 2 which means the designed antenna radiates more by an amount of 5.839 dBi in a particular direction when compared with an isotropic antenna .

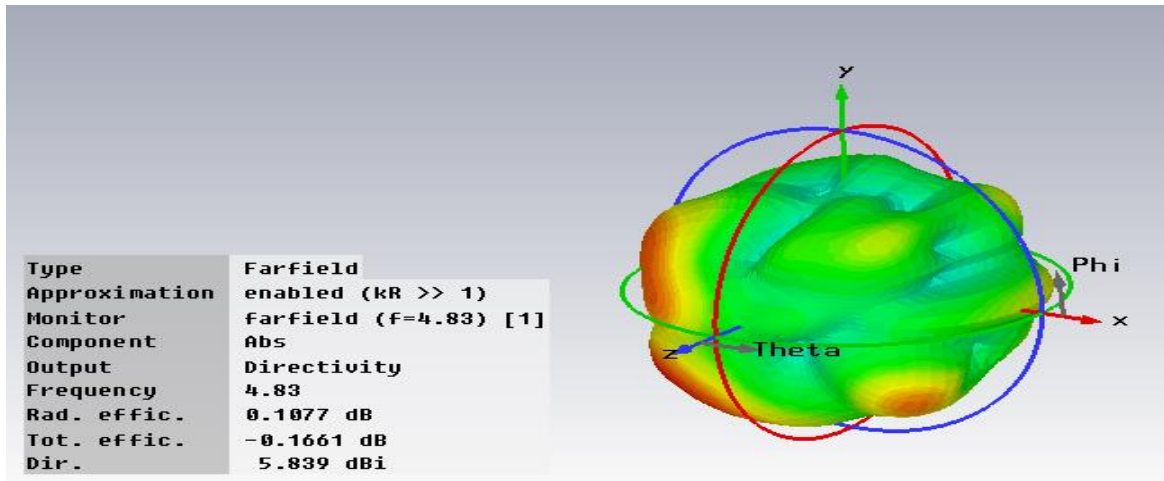


Figure 4.4 (a) Directivity (3D view) due to excitation port 1 at 4.83 GHz

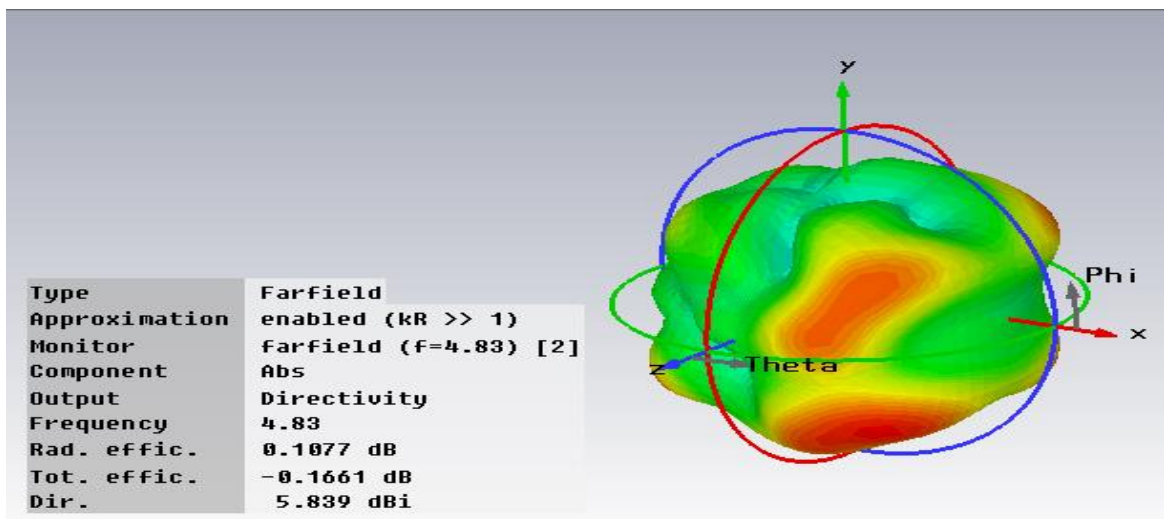


Figure 4.4 (b) Directivity (3D view) due to excitation port 2 at 4.83 GHz

#### 4.1.1.4 Current Distribution:

The current distributions due to the excitation at port 1 and 2 at 4.83 GHz is shown in figure 4.5(a) and 4.5(b) respectively. The surface current density due to both ports are shown at 4.83 GHz. From the current density value it is concluded that the surface current density due to excitation port 1 is 112.128A/m which is less than that due to excitation port 2 which is 113.44A/m which means that it is responsible for higher resonance.

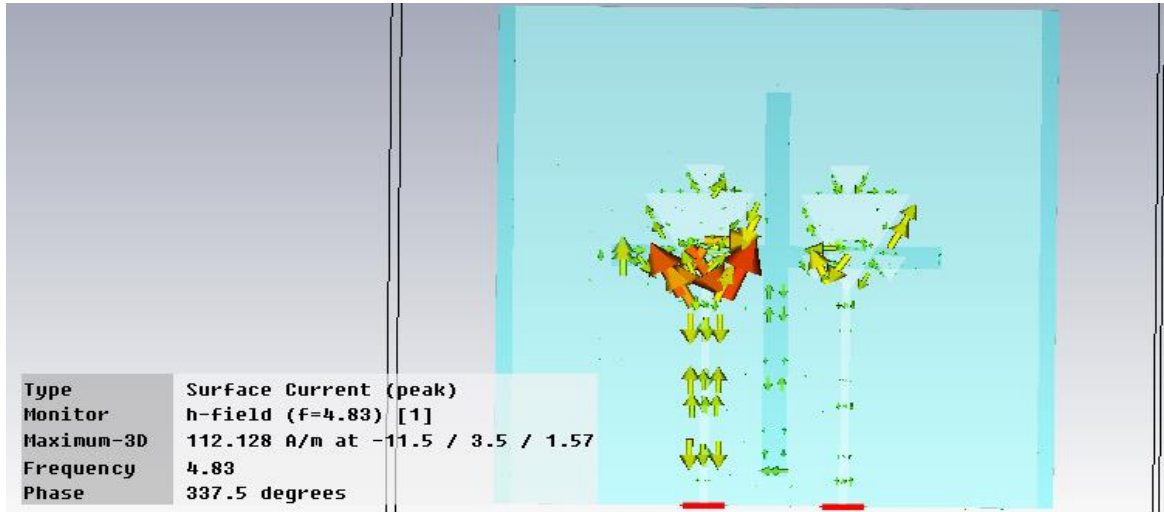


Figure 4.5 (a) Current distribution at frequency 4.83 GHz due to excitation port 1

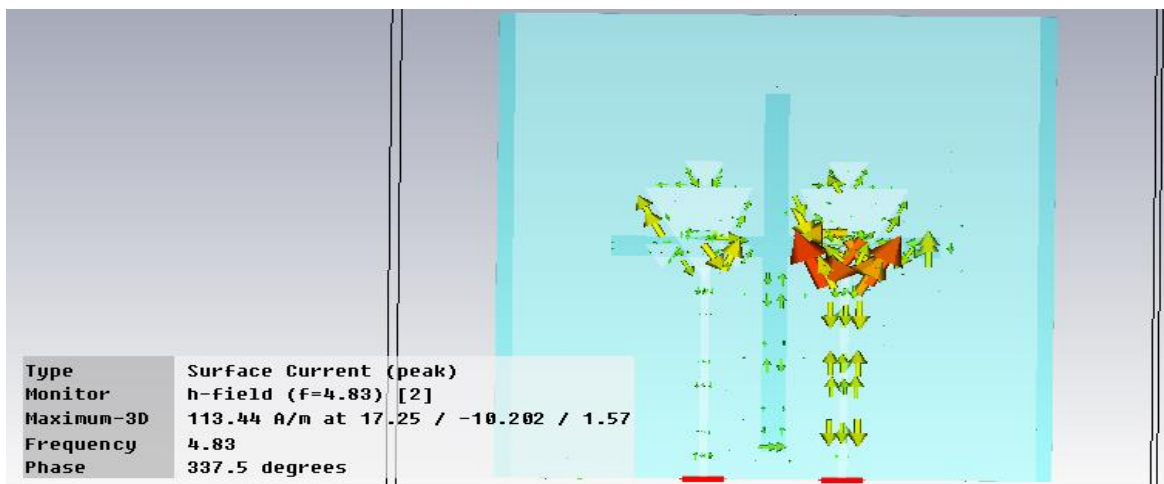


Figure 4.5 (b) Current distribution at frequency 4.83 GHz due to excitation port 2

#### 4.1.1.5 MIMO Parameters related to designed antenna array

##### 4.1.1.5a Envelope correlation coefficient

ECC tells about the independence between two antennas radiation pattern. For the two differently polarized antennas ECC is zero. ECC gives information about the radiation pattern shape, relative phase of fields between two antennas & polarization b/w the two. It is calculated by applying the scattering parameter formula given by eq. (4.1)

$$\rho = \frac{|S_{11}^* S_{12} + S_{21}^* S_{22}|^2}{(1 - |S_{11}|^2 - |S_{21}|^2)(1 - |S_{22}|^2 - |S_{12}|^2)} \quad (4.1)$$

ECC between receiving signals of different antennas should be less than 0.5. It is depicted from figure 4.6 that ECC values for the proposed two antenna MIMO system is 0.0044 and 0.04935 covering frequency band from 4.74 – 5.15 GHz.

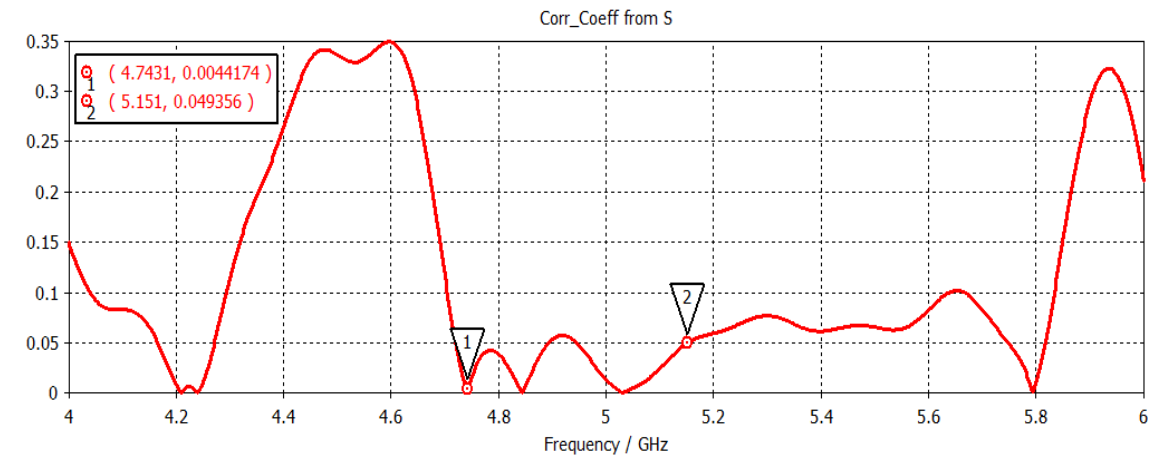


Figure 4.6 Envelope correlation coefficient at frequency 4.83 GHz

#### 4.1.1.5b Diversity gain

The diversity gain represents an increase in signal-to-interference ratio, or it gives the estimation for the reduction in transmission power when a diversity scheme is introduced, without any loss in systems performance. Figure 4.7 shows that the proposed antenna array possesses a diversity gain values of 9.99 and 9.98 covering the frequency band from 4.74 – 5.15 GHz. A good diversity gain allows a better output to be obtained in terms of SNR and thus better data rate with multiple antennas.

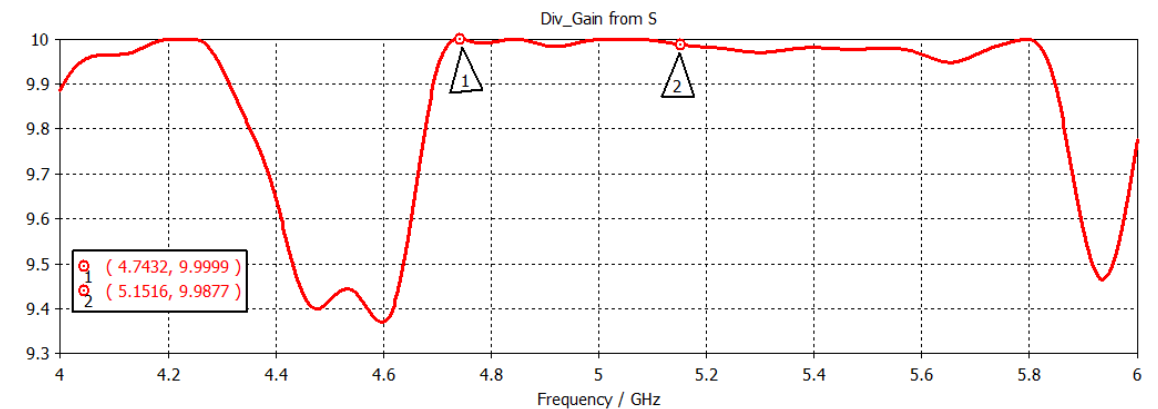


Figure 4.7 Diversity gain at frequency 4.83 GHz

#### 4.1.1.5c Capacity Analysis

In this section capacity analysis is done to analyze the applicability of the proposed antenna array. Here analysis is done considering a Rayleigh fading environment. Figure 4.8(a) shows the capacity versus bandwidth plot using equation no. (4.2) where B = Bandwidth, P = Transmitter power and  $N_0$  = Noise in the channel

$$C = B \cdot \log_2 \left( 1 + \frac{P}{N_0 B} \right) \quad (4.2)$$

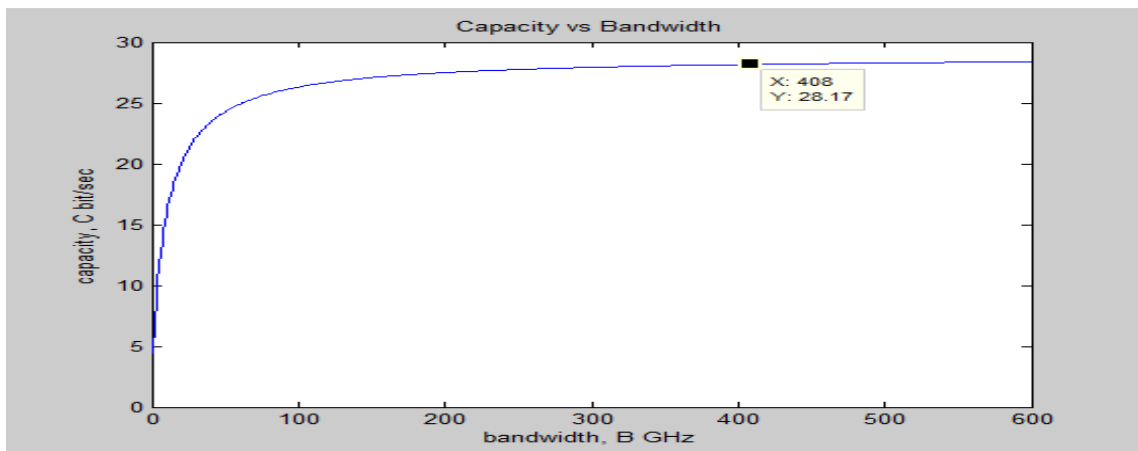


Figure 4.8 Capacity versus bandwidth plot

As can be observed from figure 4.8 with increase in frequency bandwidth, the capacity offered by the system increased. For the current antenna array designed the bandwidth offered was from 4.74 to 5.15GHz.

To improve the results of antenna array design, DGS (defected ground structure) was carried out by etching off a slot in ground plane. It is equivalent to parallel LC circuit. The current distribution in ground plane was disturbed and values of capacitance and inductance changed by varying the dimensions of slot in the ground plane. In this section DGS was obtained to get the improved results such as reduced antenna size and mutual coupling, enhanced radiation pattern for the designed antenna array.

## 4.2 Design of Compact Triangular Microstrip Patch Fractal Antenna Array with Defected Ground Structure for MIMO Applications

Since a DGS helps in improving the antenna performance, this section presents the design of a fractal triangular antenna array with DGS. The structure is designed using equation no. 14, fractal shapes of second order are cut from the patch to give it a sierpinski gasket fractal antenna geometry. Figure 4.8 shows the geometry of patch antenna. The structure is a compact triangular microstrip patch fractal antenna array with defected ground plane and feed line. The antenna design was optimized using CST MWS V'10 and all the parameters are mentioned in table 4.3.

Table 4.3 Design Specifications of Single Band Antenna

Frequency (fr)	5.6GHz
Dielectric Constant ( $\epsilon_r$ )	4.4
Patch Substrate Thickness	1.57mm
Feed Substrate Thickness	1.57mm

Table 4.4 Optimized Dimensions of the Triangular patch fractal Antenna Array

Parameters	$s$	$L_g$	$W_g$	$L_f$	$W_f$	$L_d$	$W_d$
<b>Description</b>	Patch side	Length of Ground	Width of Ground	Length of Feedline	Width of Feedline	Length of DGS	Width of DGS
Values	34.5 mm	136 mm	136 mm	60.3mm	1.25mm	80mm	10mm

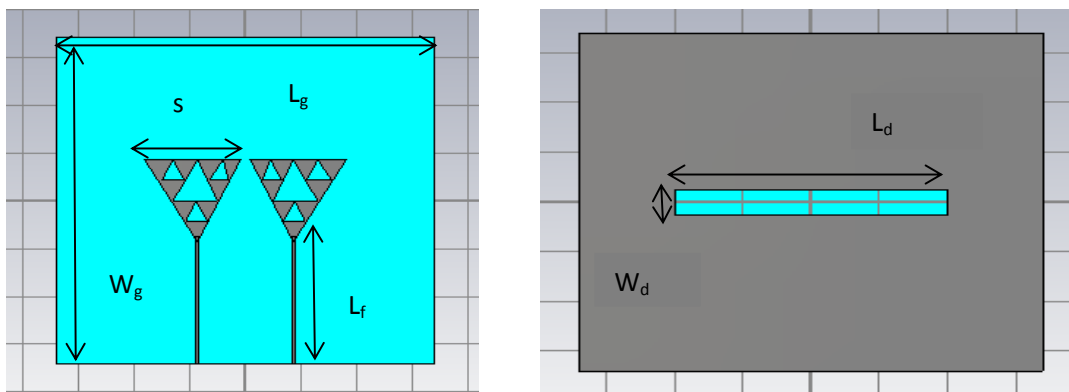


Figure 4.9 (a) Front view of proposed Antenna (b) back view of proposed antenna designed on CST microwave studio

### 4.2.1 Simulation Setup and Result of Antenna

Designs and simulations of proposed antenna are done using CST MWS V'10. The simulation results are mentioned in further sections.

#### 4.2.1.1 Return loss and Smith Chart

Return loss [ $S_{11}$  in dB] of the triangular patch antenna array is shown in figure 4.9. The antenna shows a resonant frequency of 5.68GHz with peak return loss of -48dB and bandwidth obtained is 74.12%. The higher value of the return loss indicates better coupling which leads to higher value of the directivity and more gain for the antenna designed. The antenna shows a -10dB impedance bandwidth from 5.43 – 5.848GHz. Figure 4.9(a) shows the  $S_{11}$  plot of iteration for the first order fractal antenna which gives multiple resonance and figure 4.9(b) shows the parameter plot of the antenna with  $S_{11}$ ,  $S_{12}$  &  $S_{22}$ . Plot of  $S_{11}$  with respect to frequency shows that the antenna is resonant at frequency of 5.6 GHz and bandwidth of 418 MHz. This is second iteration plot which is optimized.

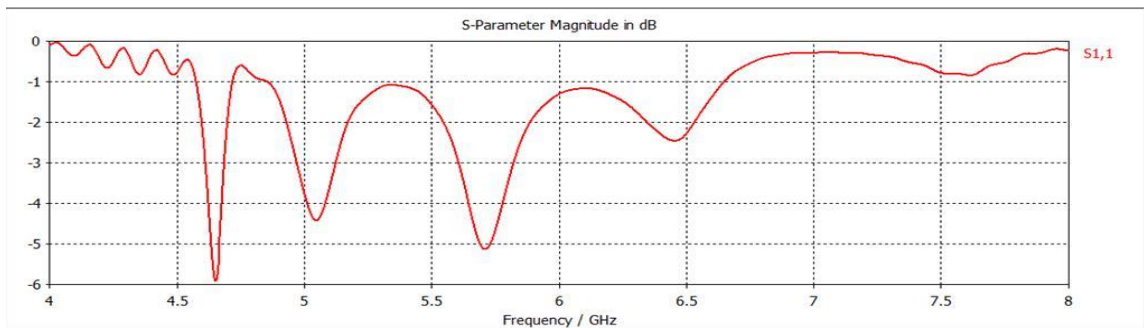


Figure 4.10(a) Return Loss  $S_{11}$  (in dB) of Simulated First Order Fractal Antenna

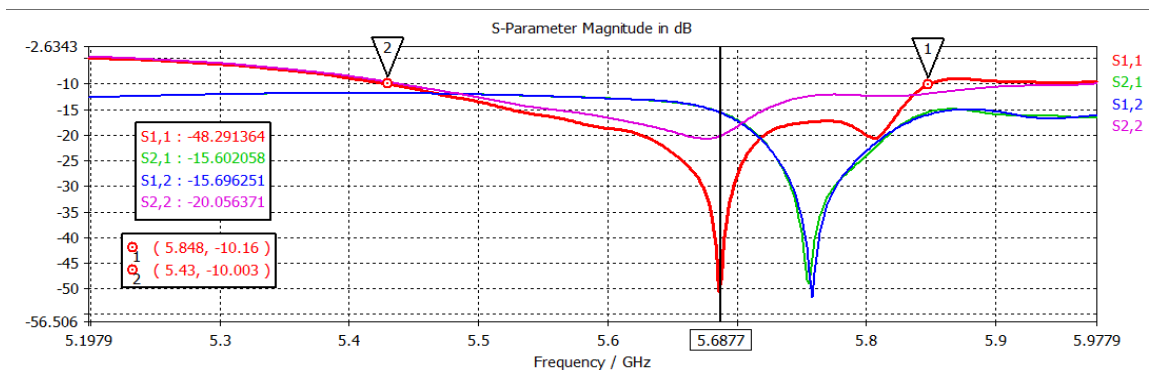


Figure 4.10 (b) Return Loss  $S_{11}$  (in dB) of Simulated second order fractal Antenna at 5.6GHz

#### 4.2.1.2 Smith Chart and Antenna Impedance

Smith chart for the proposed antenna is shown in the figure 4.10. The antenna is matched to an impedance of 50 ohms at the desired band of operation from 5.43 – 5.848 GHz.

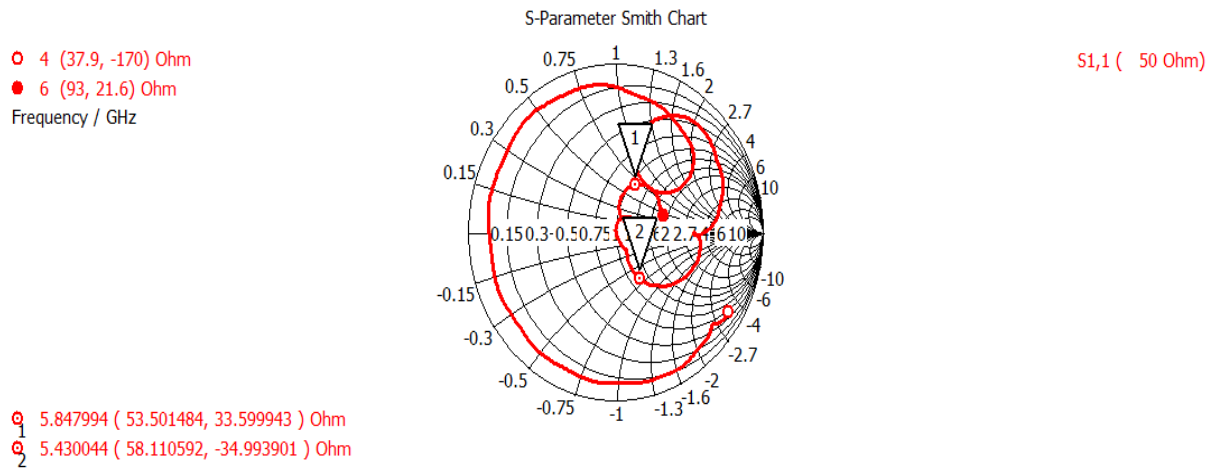


Figure 4.11 Smith Chart at 5.6GHz

#### 4.2.1.3 Directivity

Figure 4.11 shows the 3D directivity plot of the antenna. It represents that the antenna resonating at 4.83 GHz provides a directivity value of 6.554 dBi when the excitation is given to port 1 and value of directivity is 6.521 dBi when excitation is given to port 2 which means the designed antenna radiates more by an amount of 6.554 dBi in a particular direction when compared with an isotropic antenna which radiates equally in all directions.

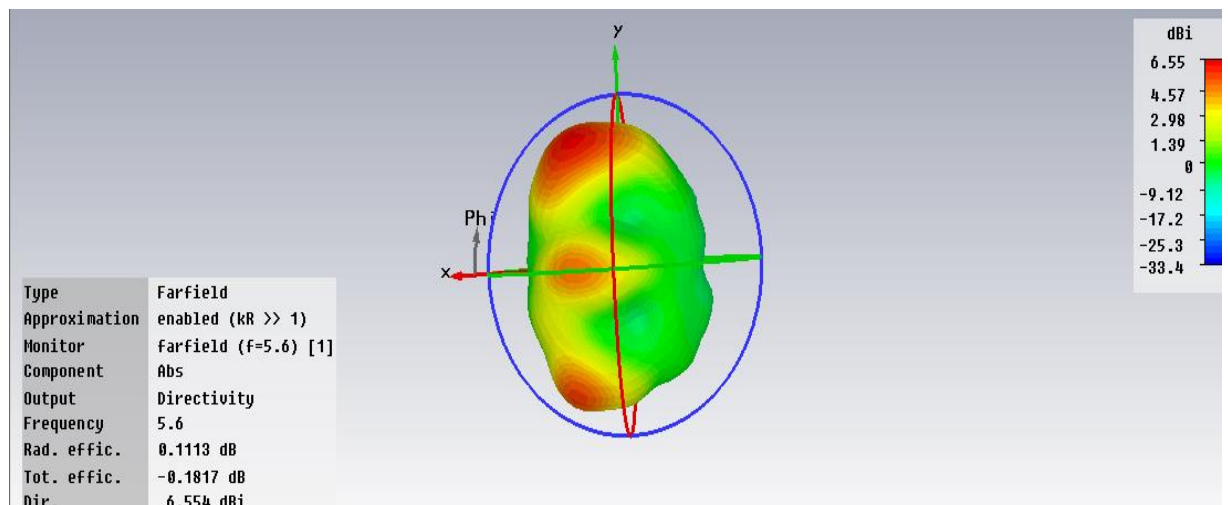


Figure 4.12 (a) Directivity (3D view) due to excitation port 1 at 5.6 GHz

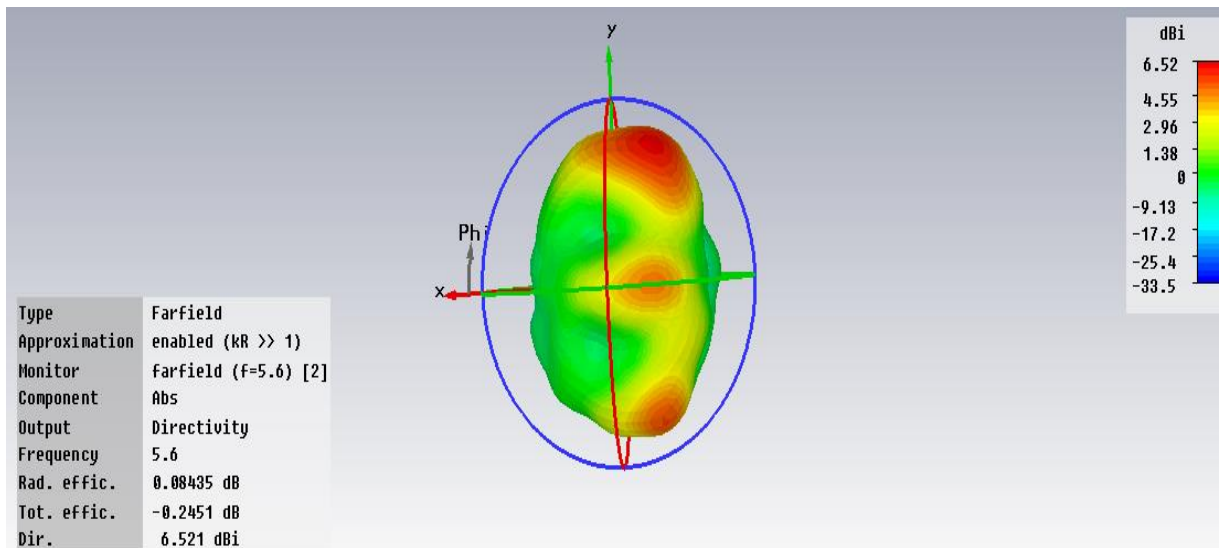


Figure 4.12 (b) Directivity (3D view) due to excitation port 2 at 5.6 GHz

#### 4.2.1.4 Current Distribution:

The current distributions due to the excitation port 1 &2 at 5.6 GHz is shown in figure 4.12(a) and 4.12(b) respectively. The surface current density due to both ports are shown at 5.6 GHz. From the current density value it is concluded that, surface current density due to excitation port 1 is 29.8552A/m which is less than that due to excitation port 2 which is 27.2919A/m which means that it is responsible for higher resonance.

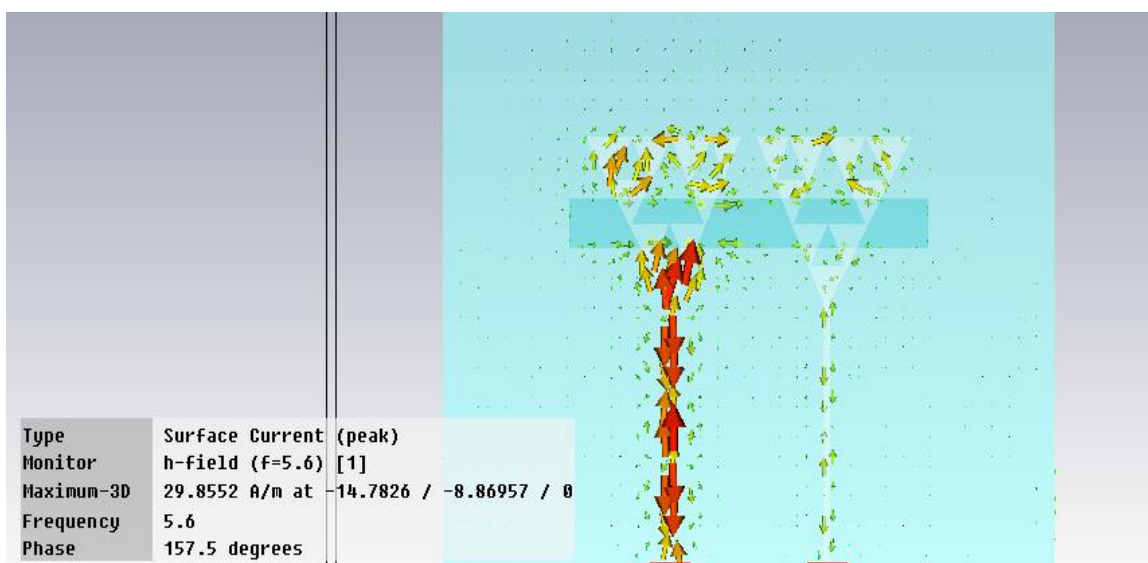


Figure 4.13 (a) Current distribution at frequency 5.6 GHz due to excitation port 1

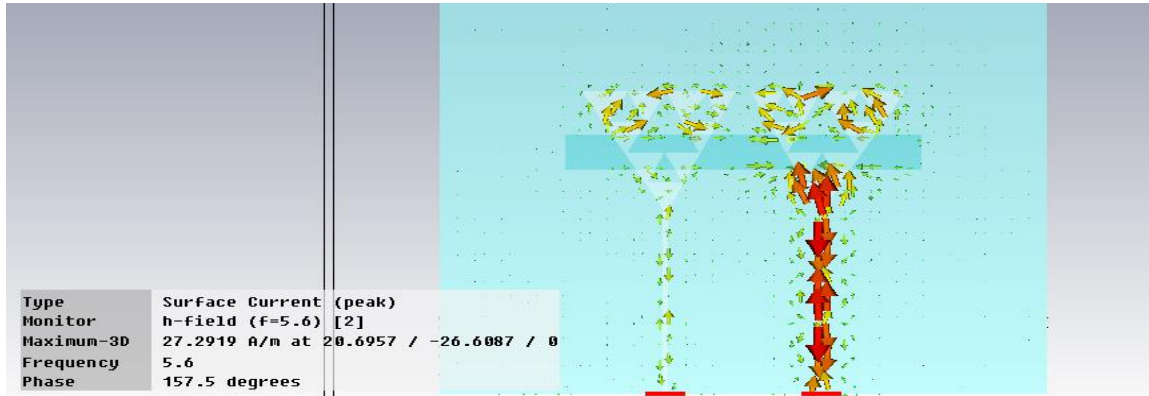


Figure 4.13 (b) Current distribution at frequency 5.6GHz due to excitation port 2

#### 4.2.1.5 MIMO Parameters related to designed antenna array

##### 4.2.1.5a Envelope Correlation coefficient

ECC is calculated using equation no. (4.1), it shows how two or more antenna in an antenna array affect each other's performance. This value should be ideally zero but a value less than 0.5 is satisfactory. It is depicted from fig 4.13 that ECC for the proposed two antenna MIMO system is 0.0625 at resonating frequency of 5.6GHz.

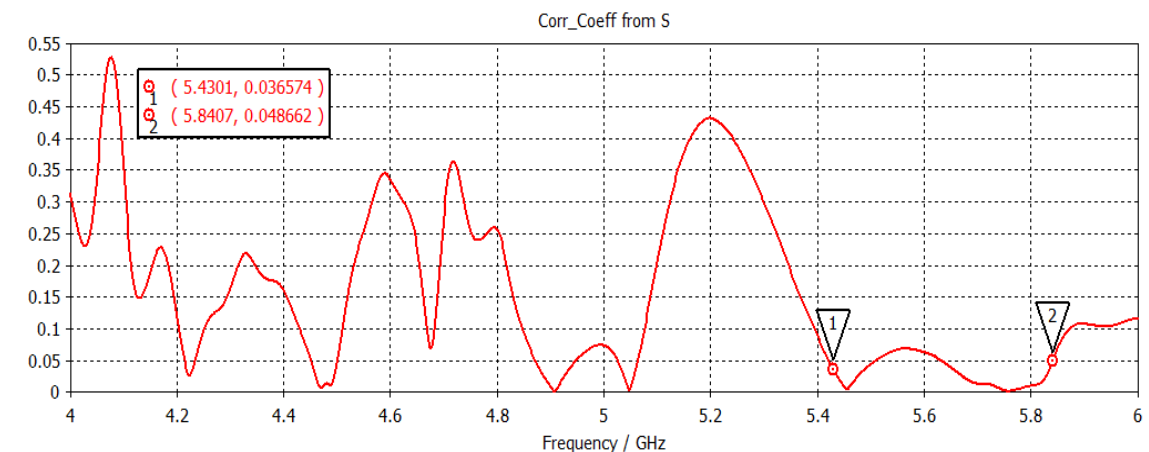


Figure 4.14 Envelope Correlation coefficient at frequency 5.6 GHz

##### 4.2.1.5.2 Diversity gain

The diversity gain represents an increase in signal-to-interference ratio, or it gives the estimation for the reduction in transmission power when a diversity scheme is introduced, without any loss in system's performance. Figure 4.14 shows that the proposed antenna array possesses diversity gain of 9.98 at the resonant frequency of 5.6 GHz of antennas operation.

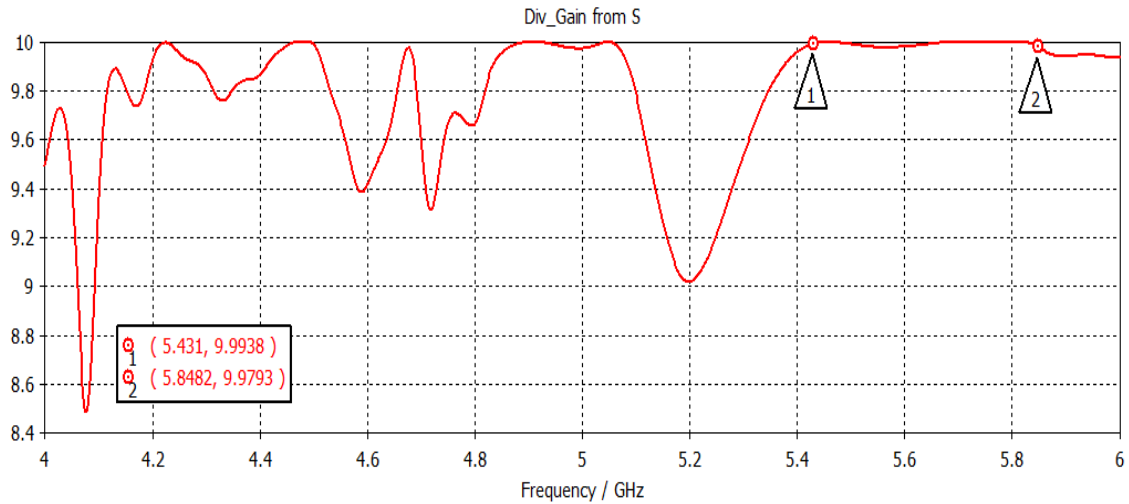


Figure 4.15 Diversity gain at frequency 5.6 GHz

#### 4.1.2.5.3 Capacity Analysis

In this section capacity analysis is done to analyze the applicability of the proposed antenna array. Here analysis is done considering a Rayleigh fading environment. Figure 4.16(a) shows the capacity versus bandwidth plot using equation no. (4.2) where  $B$  = Bandwidth,  $P$  = Transmitter power and  $N_0$  = Noise in the channel

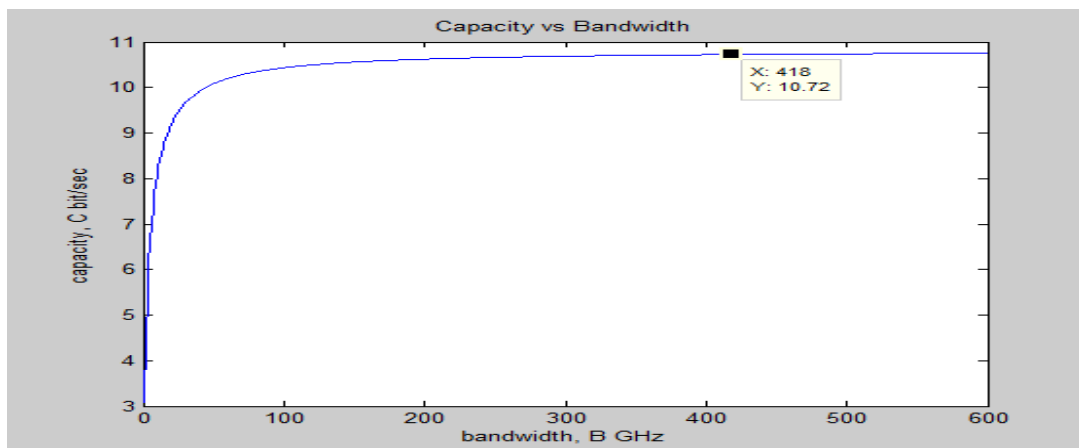


Figure 4.16 Capacity versus Bandwidth plot

As can be observed from figure 4.8 with increase in frequency bandwidth, the capacity offered by the system increased. For the current antenna array designed the bandwidth offered was from 5.43 to 5.848GHz.

#### Conclusion:

This chapter presents the design of two wide band MSA arrays for WLAN applications. The first design is regarding a complementary triangular MSA array & the second design is

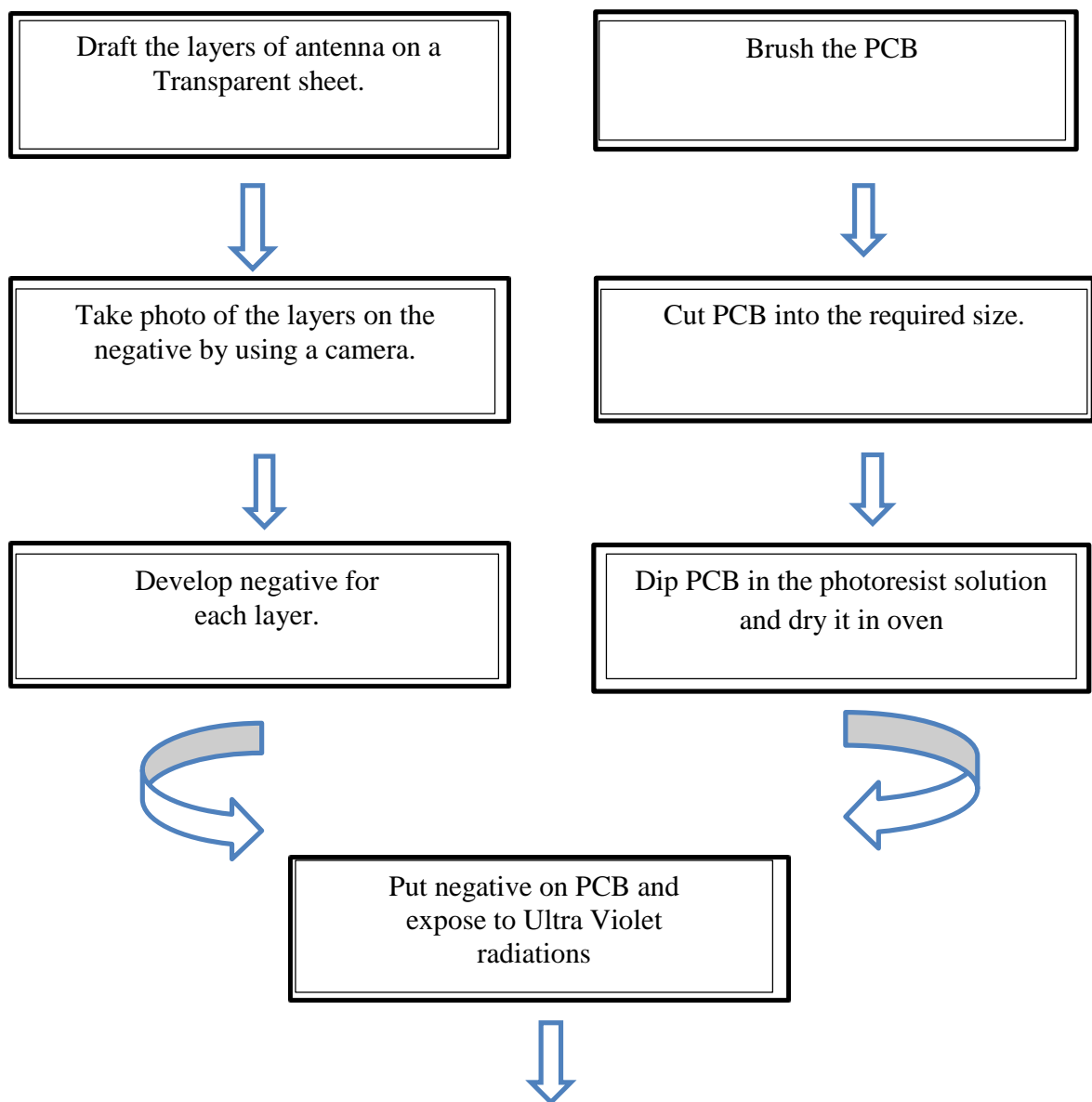
regarding a compact fractal triangular MSA array as triangular pattern gives a higher impedance bandwidth and compactness in size as compared to a rectangular patch antenna with microstrip feed. The antenna shows a gain of 5.839 dBi and 6.55 dBi respectively for WLAN application.

## Chapter 5

### Fabrication and Testing of Proposed Microstrip Antenna Array

#### 5.1 Fabrication process:

Various steps followed in the fabrication of an antenna which can be shown via a flow chart:



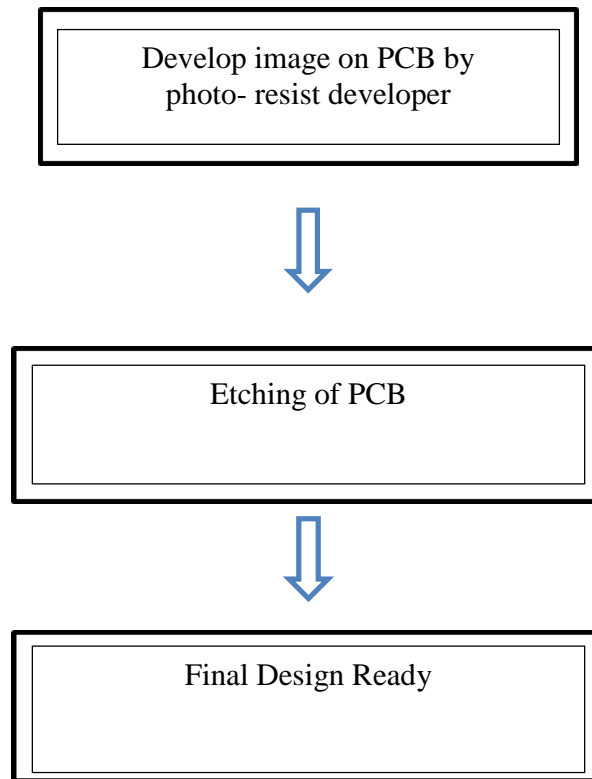


Figure 5.1 Fabricate Flow of PCB Design

### 5.2 Instruments used for fabricating a microstrip Patch antenna:

The hardware used for the antenna consists of two processes which are PCB (Printed circuit board) design and testing of the antenna. Following are the steps for the PCB design:

- Negative developing: The negative development is done by software. The whole design is designed in this software and then print out of that design is taken.
- The PCB cutter is used to cut PCB's as per desired size. The actual size of antenna i.e. Substrate size of material, like FR4 ( $\epsilon_r = 4.4$ ) is used here. Figure 5.4 shows the PCB cutter.



Figure 5.2 PCB cutter

- Operations on PCB: Now the PCB is dipped once in the photo resist developer placed in yellow light. It dried in an oven for 3-5 minutes.



Figure 5.3 PCB Coating Unit

The oven unit is used to dry the final design on antenna, which contain the paint on the layer that protects the copper to clean up. Thus, the oven dries the PCB at 140-150 degree temperature properly. Figure 5.6 shows the picture of the Oven Unit.



Figure 5.4 Oven Unit

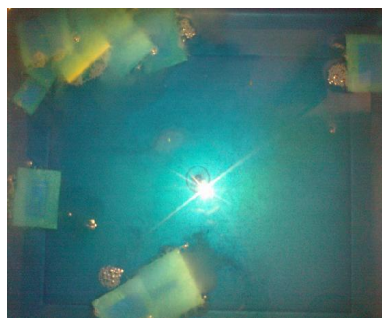


Figure 5.5 Etching Unit

### 5.3 Fabricated Antenna Arrays

The images of fabricated antennas are shown in figure 5.8 and 5.9. Figure 5.8 shows the wide band complementary sierpinski gasket fractal antenna array with reduced ground structure. Figure 5.9 shows the sierpinski gasket triangular patch microstrip antenna array

with reduced ground structure and both are the fabricated microstrip antennas with microstrip feed.



Figure 5.6 (a) Patch with microstrip feed line (b) DGS on ground plane

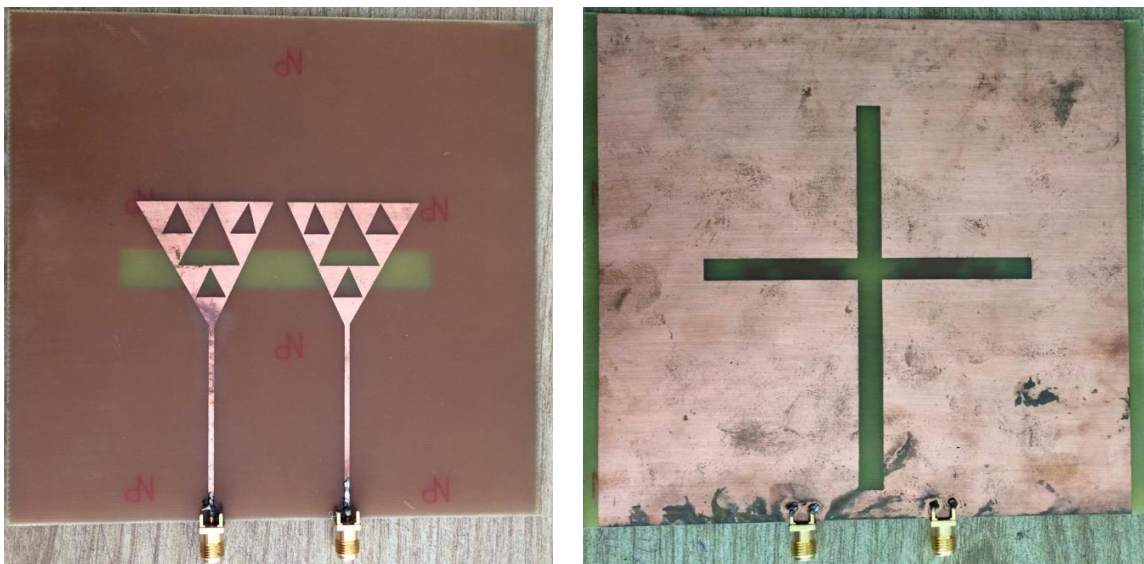


Figure 5.7 (a) Patch with microstrip feed line (b) DGS on ground plane

In these figures, the material used for fabrication antenna is PEC (Copper) of height 0.035mm.

#### 5.4 Testing of Antennas on VNA:

A microstrip feed single band triangular patch microstrip antenna at 4.83 GHz and 5.6GHz for WLAN application were designed using CST2010 studio (software). But practically, antenna has been tested using VNA model no: E5071C, frequency range is 9KHz-8.5GHz and is shown below:



Figure 5.8 VNA used for testing

#### 5.4.1 Simulated and Measured Results of Antenna Arrays

This section gives the simulated and measured results for the complementary sierpinski gasket fractal antenna array that resonates at 4.38GHz.

##### Simulated Results of the Antennas

The simulated results of the antennas discussed in chapter 5 have been discussed below:

- **Broad Band Antenna at 4.8 GHz:**

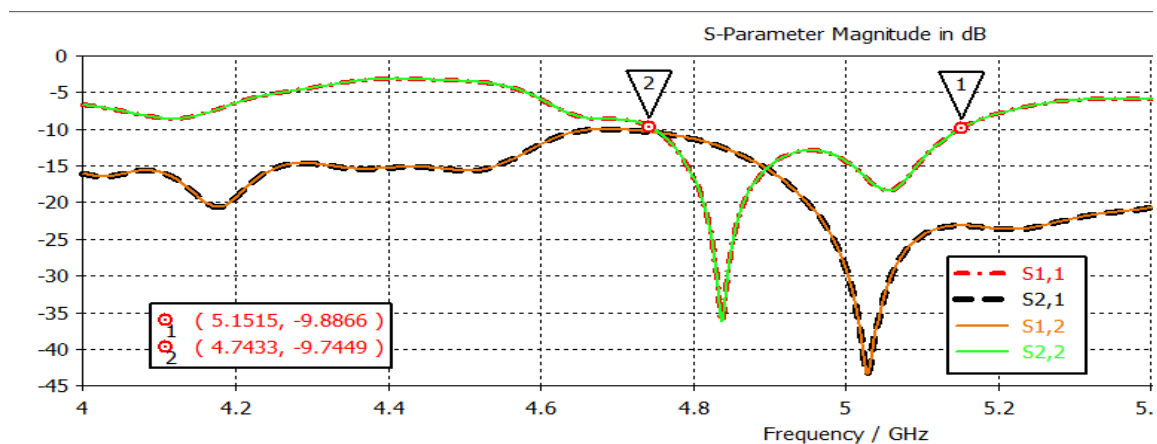


Figure 5.9 Return Loss S11 (in dB) of Simulated Complementary Sierpinski Antenna at 4.83GHz

- **Broad Band Antenna at 5.6 GHz:**

Figure 5.2 shows the  $S_{11}$  results of fractal triangular antenna array.

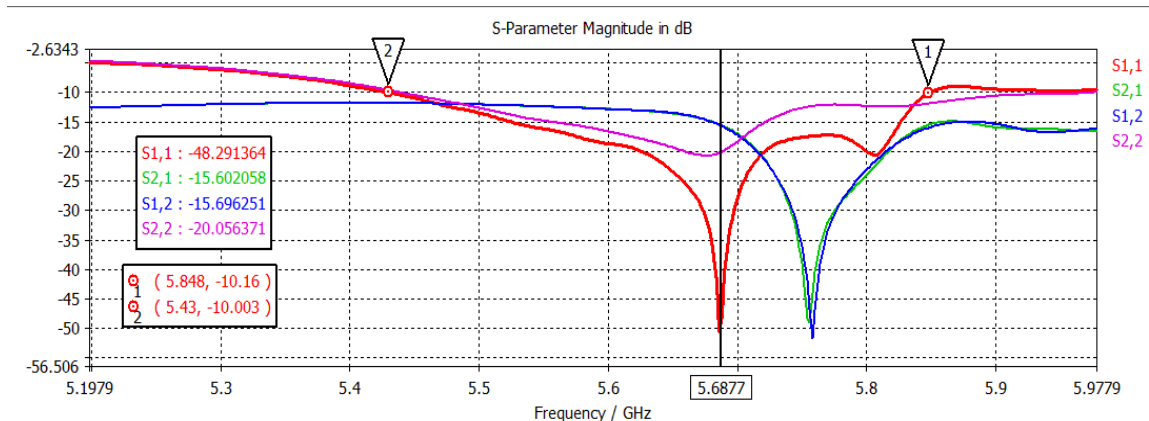
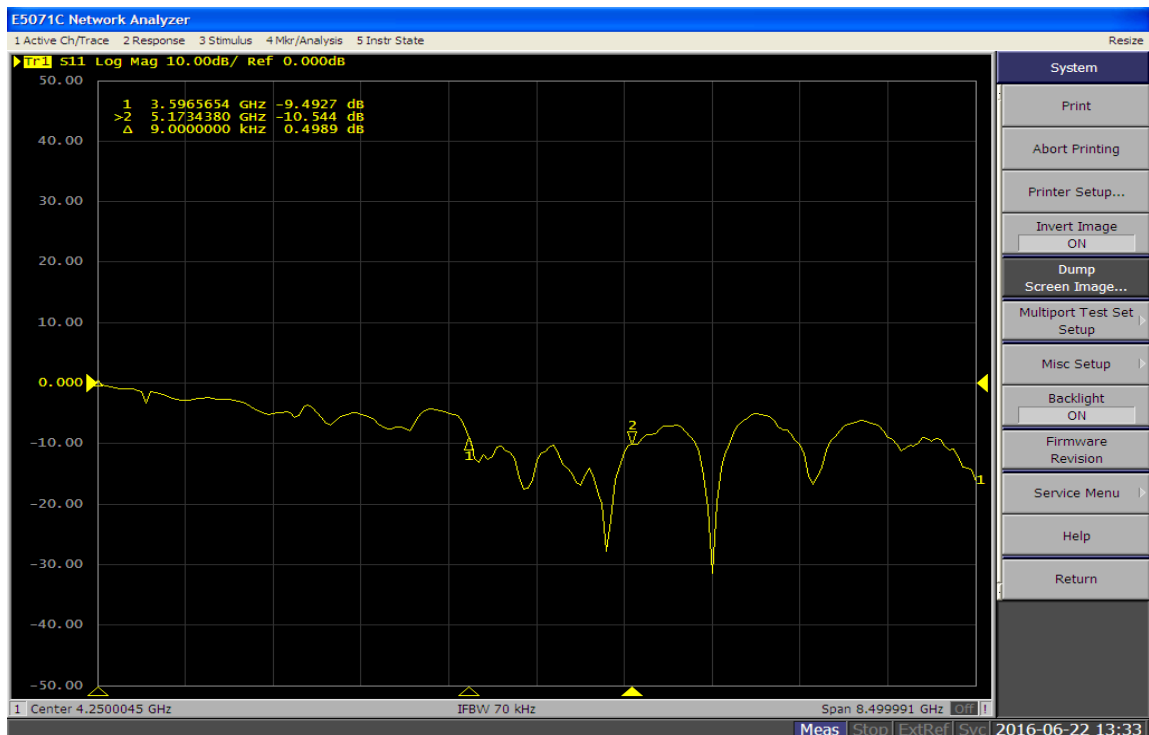


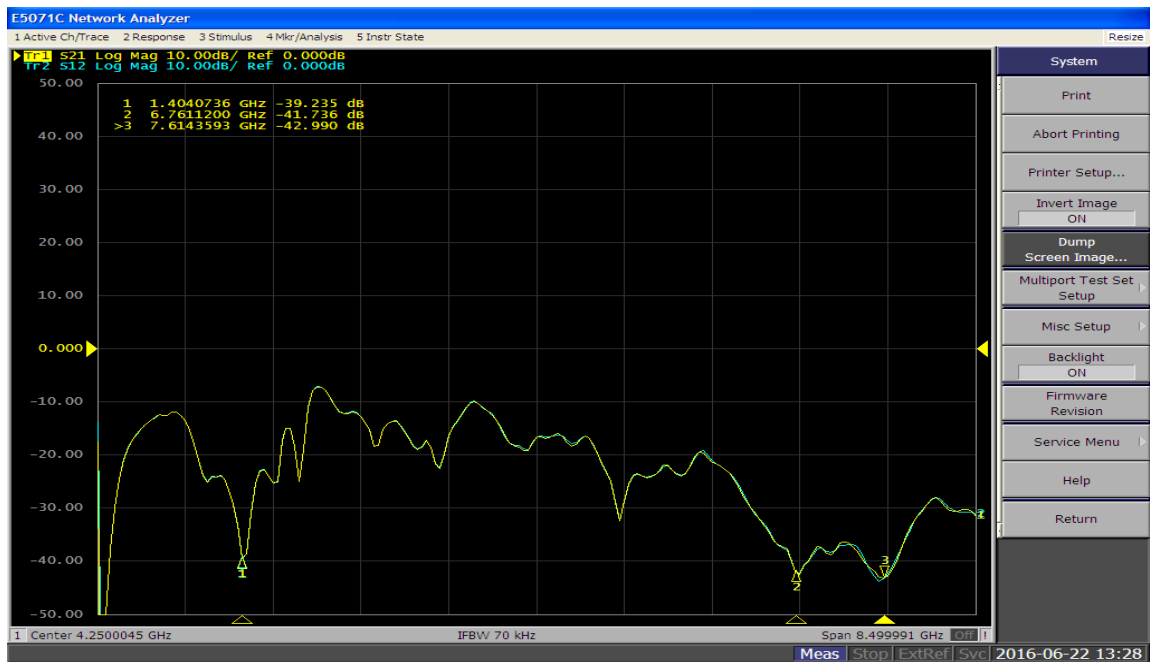
Figure 5.10 Return Loss  $S_{11}$  (in dB) of Simulated Antenna at 5.6GHz

Figure 5.11 shows the measured results of the complementary sierpinski gasket fractal antenna array frequency and covers the range from 3.596GHz to 5.17GHz. Thus bandwidth formed is 1574MHz i.e. wide band covered by antenna, useful for C-band applications.

Figure 5.11 shows the graph at 4.38GHz.



(a)



(b)

Figure 5.11 (a), (b) Tested results at 4.38GHz

Table 5.1 Comparison between Simulated results and fabricated results of Complementary Sierpinski Gasket Fractal Antenna Array

Parameters	Simulated Results	Fabricated Results
Frequencies Covered	4.74GHz to 5.15GHz	3.59GHz to 5.17GHz
Return Loss	-36.059dB	-17dB
Transmission Loss	-44dB	-20dB
Bandwidth	408.2MHz	1574MHz
Applications covered by complementary antenna	C- band applications	Covering applications of C-band also used in military applications covering the bands from 4.74 GHz to 5GHz

The measured results for the compact triangular patch microstrip antenna array that resonates at 5.45GHz frequency and covers the range from 5.38GHz to 5.52GHz. Thus

bandwidth formed is 140 MHz i.e. band covered by antenna, useful for WLAN application.

Figure 5.12 shows the graph at 5.45GHz.

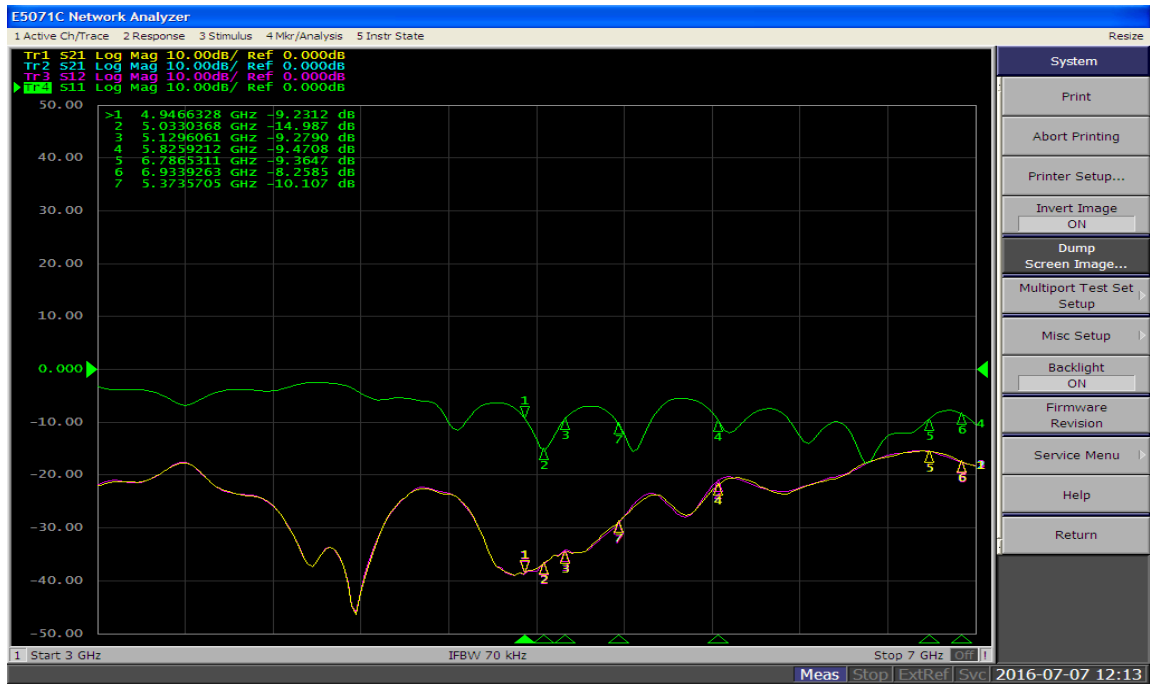


Figure 5.12 Tested results at 5.45GHz

Table 5.2 Comparison between Simulated results and fabricated results of Compact Triangular Patch Antenna Array

Parameters	Simulated Results	Fabricated Results
Frequencies Covered	5.43GHz to 5.848GHz	5.38GHz to 5.52Ghz
Return Loss	-48.291dB	-15dB
Transmission Loss	-52dB	-15dB
Bandwidth	418MHz	140MHz
Applications covered by Fractal antenna	Covers a large range of frequencies, covering WLAN applications at 5.8GHz	Covering applications of WLAN at 5.2GHz

#### **5.4.2. Discussion of results**

It was found that the results have some variations given below:

- In the single wide band complementary antenna, the simulated results covers the frequency band from 4.7GHz to 5.15GHz and in the fabricated results , antenna shifts to left and covers the frequency band 3.59GHz to 5.17Ghz.
- In the another wide band fractal antenna , the simulated results covers the frequency bands 5.43 GHz to 5.848GHz and in the fabricated results, antenna shifts to the left and covers the frequency band 5.38 GHz to 5.52 GHz and resonant frequencies have shifted in the magnitude from the designed frequency.

FR-4 board could be one of the reasons for shift. The other factors affecting the results and shift in the resonant frequency are chemical used, surface finish and metallization thickness

## Chapter 6

### Conclusion and Future work

---

#### 6.1 Conclusion

- In the report, firstly a microstrip feed slotted rectangular patch single band antenna was Designed which resonates at 5.138 GHz and gives a bandwidth of 141 MHz, therefore antenna can be used for the WLAN applications(C band). The physical parameters inspected are the substrate used and their dielectric constant, feed line and ground plane, patch with slot on it. The antenna parameters like operating frequency, input impedance, VSWR, Bandwidth, Return loss, and directivity are calculated for each antenna configuration.
- Secondly a single band antenna slotted triangular patch antenna using microstrip feed was designed which resonates at frequency 4.83GHz and provides a single band having bandwidth of 169MHz.
- A wide band complementary gasket fractal antenna was designed which resonates at frequency of 4.838 GHz and provides a wide bandwidth of 408.2 MHz. The directivity and gain of the proposed antenna obtained are good to be used for WLAN Applications. The simulated antenna in chapter4 were fabricated and tested and the fabricated results were somewhat different from the simulated results. In the wide band complementary antenna array the resonating frequency shifted from 4.83 GHz to 4.38 GHz, also the bandwidth of the fabricated antenna is more than that of simulated antenna.
- A wide band Triangular patch fractal antenna was designed which resonates at frequency of 5.6 GHz and provides a wide bandwidth of 418 MHz. The simulated antenna in chapter4 were fabricated and tested and the fabricated results were somewhat different from the simulated results. In the single band antenna, the resonating frequency shifted from 4.8 GHz to 4.38 GHz, also the bandwidth of the fabricated antenna is more than that of simulated antenna. The bandwidth of the fabricated antenna is also increased as compared to simulated antenna.

Table 6.1 Concluded results of the designs

Designs	Return loss	Resonant frequency	Directivity	Bandwidth
Single band slotted rectangular patch MSA	-19.27dB	5.13GHz	6.401dBi	141MHz
Single band slotted triangular patch MSA	-25.548dB	4.83GHz	6.583dBi	169MHz
Wide band complementary sierpinksi gaket fractal array	-36.059dB	4.83GHz	5.839dBi	408.2MHz
Wide band triangular patch fractal array	-48dB	5.68GHz	6.55dBi	418MHz

## 6.2 Future Scope

The antennas designed in this thesis report are used in various applications like C-Band, WLAN, Microwave applications communications etc.

Various techniques can also be used in future to design antenna which are as follows:

- **Electromagnetic band gap structure (EBG):** Electromagnetic Band Gap (EBG) substrates can be used for patch antennas so that they can minimize the effect of surface waves significantly with respect to frequency and are able to provide relatively broadband frequency performance.
- **Metamaterials:** It is a metallic or semiconductor substance and its properties varies with inter-atomic structure. There are few metamaterials with the tendency of bending the visible light rays in the direction opposite from refractive media. Some metamaterials show such behavior at infrared (IR) wavelengths. There are some possible applications of transparent metamaterials with negative indices of refraction which are IR lasers, spectrometry, optical communications systems, medical diagnostic equipment and optical cloaking devices. Gain enhancement of the triangular patch antenna can be achieved by obtaining circular polarization for the antenna structure. It amplifies gain of antenna without affecting antenna height and back radiation.

- **Other feeding techniques:** the other feeding techniques of microstrip patch antenna like co-axial feeding, aperture coupling and CPW can also be used in future to design microstrip patch antenna

### **List of Publications**

- Sheifali Gupta, Dr. Amanpreet Kaur, “**Design of Compact Triangular Microstrip Patch Fractal Antenna Array for MIMO Applications**”, IJAMT, Vol 1, NO.1, May2016.
- Sheifali Gupta, Ayushi Agarwal, Dr. Amanpreet Kaur, “**Design of Dual Frequency Compact Triangular Patch Array for MIMO Applications**”, IJEAST, Vol 1, NO.6, April-May 2016.
- Sheifali Gupta, Ayushi Agarwal, Dr. Amanpreet Kaur, “**FDTD Analysis of Triangular Patch Antenna**”, ICMARS, Dec. 2015.
- Sheifali Gupta, Dr. Amanpreet Kaur, “**A Review paper on Triangular Patch MIMO Antenna for wireless communications**”, RIECEE, May 2015.

## REFERENCES

- [1] L. Hanlen and A. Grant ,” Capacity Analysis of Correlated MIMO Channels”, *IEEE Transactions on Information Theory*, Vol. 58, NO. 11, November 2012
- [2] A. Goldsmith , S.A. Jafar , N. Jindal and S. Vishwanath ,”Capacity Limits of MIMO Channel”, *IEEE Journal on Selected Areas in Communication* ,Vol.21 , NO. 5, June 2003
- [3] C.A.Balanis. *Antena Theory:Analysis and Design* , 2<sup>nd</sup> ed. United States of America , John Wiley&Sons Inc.,1997.
- [4] F. Y. Zulkifli, Daryanto and E. T. Rahardjo , “Slot Ring Triangular Patch Antenna with Stub for MIMO 2x2 Wireless Broadband Application ,” *Antenna Propagation and Microwave Research Group (AMRG)*,Vol 02 ,pp. 885-887,2013
- [5] R. G. Vaughan and J.B Andersen, “Antenna Diversity in Mobile Communications,” *IEEE Transactions on Vehicular Technology*,36,4, pp.149-172,1987 .
- [6] N. Kumprasert and W. Kiranon , “Simple and Accurate Formula for the Resonant Frequency of the Equilateral Triangular Microstrip Patch Antenna , ” *IEEE Transactions on Antennas and Propagation*, Vol. 42, NO. 8,pp. 1178-1179, 1994
- [7] A.A. Rasheed and G. Kumar , “Single Feed Circularly Polarized Modified Triangular Microstrip Antennas ,”*IEEE Transactions on Antenna and Propagation* ,Vol.2, pp.818-821, 1994
- [8] R. R. Ramirez and F. D. Flaviis , “Triangular Microstrip Patch Antennas for Dual Mode 802.11 a,b WLAN Application , ” *IEEE Transactions on Antenna and Propagation*,Vol.4,pp. 44-47, 2002
- [9] S. Blanch, J. Romeu, and I. Corbella, “Exact representation of antenna system diversity performance from input parameter description,” *Electron. Lett.*, vol. 39, no. 9,pp.705-707, 2003.
- [10] J. S. Kuo and G.B. Hsieh, “ Gain Enhancement of a Circularly Polarized Equilateral Triangular Microstrip Antenna With a Slotted Ground Plane ,” *IEEE Transactions on Antennas and propagation* , Vol. 51, No.7, pp.1652-1656, 2003

- [11] R K Vishwakarma , J A Ansari and M K Meshram , “Equilateral Triangular Microstrip Antenna for circular polarisation dual band operation ,”*Indian Journal of radio and space physics* , Vol. 35 , pp. 2006
- [12] J.S. Row and Y.Y.Liou , “ Broadband Short-circuited Triangular Patch Antenna ,” *IEEE Transactions on Antennas and Propagation*,AP-54,7,pp. 2137-2141, 2006
- [13] B. Clerckx ,C. Craeye , D. V. Janvier, and C. Oestges, “Impact of Antenna Coupling on 2\*2 MIMO Communications,” *IEEE Transactions on Vehicular Technology*,Vol.56,3, pp.1009-1018,2007.
- [14] F. Y. Zulkifli, S. T. Lomorti and E. T. Rahardjo , “ Improved Design of Triangular Patch Linear Array Microstrip Antenna Using Isosceles-Triangular Defected Ground Structure ,” *Proceedings of Asia-Pacific Microwave Conference* ,pp1-4,2007
- [15] S.Ranvier ,C. Luxey , P. Suvikunnas , R. Staraj and P. Vainikainen , “Capacity Enhancement by Increasing Both Mutual Coupling and Efficiency: a Novel Approach ,” *IEEE Transactions on Antennas and propagation*, pp. 3632-3635,2007
- [16] C. A. Tunc, D. A. Vakur , B. Erturk, and A. Altintas, “Capacity of Printed Dipole Arrays in the MIMO Channel , ” *IEEE Antennas and Propagation Magazine*, Vol. 50, No. 5,pp.190-198, 2008
- [17] H. Zhang, Z. Wang, J. Yu, and J. Huang , “A Compact MIMO Antenna for Wireless Communication,” *IEEE Antennas and Propagation Magazine*, Vol. 50, No.6,pp. 104-107,2008
- [18] L. H. Weng, Y. C. Guo, X. W. Shi, and X. Q. Chen , “An Overview on Defected Ground Structure ,” *Progress In Electromagnetics Research B*, Vol. 7, pp.173-189, 2008
- [19] F. Y. Zulkifli, E. T. Rahardjo, and D. Hartanto , “ Radiation Properties Enhancement of Triangular Patch Microstrip Antenna Array Using Hexagonal Defected Ground Structure,” *Progress In Electromagnetics Research M*, Vol. 5 ,pp.101-109, 2008
- [20] A. Ocalan, A. Savascihabes, B.Gorgec, O. Ertug and E. Yazgan , “Compact Space- Multimode Diversity Stacked Circular Microstrip Antenna Array for

- 802.11n MIMO-OFDM WLANs ,” *Loughborough Antennas & Propagation Conference*, pp. 525-528,,2009
- [21] C.A. Tunc, U. O. Vakur ,B. Ertirc, and A. Altintas, “On the Capacity of Printed Planar Rectangular Patch Antenna Arrays in the MIMO Channel: Analysis and Measurements,” *IEEE Antennas and Propagation Magazine*, Vol.52, No. 6, pp. 181-192,2010
- [22] C. Peixeiro , “Microstrip Patch Antennas ,” *IEEE Transactions on Antennas and Propagation*, pp. 684-688, 2011.
- [23] H. Li, X. Lin , B. Lau and S. He , “Equivalent Circuit Based Calculation of Signal Correlation in Lossy MIMO Antennas ,” *IEEE Transactions on Antennas and propagation*, Vol. 61, No. 10,pp. 5214-5222,2013
- [24] T. Gunasekaran, N. Veluthambi, P. Ganeshkumar and K.R.S.Kumar, “Design of Edge Fed Microstrip Patch Array Antenna Configurations for WiMAX ,” *IEEE Transactions on Antennas and propagation*, 2013
- [25] A. Reineix and B.D Jecko , “Analysis of Microstrip Patch Antennas using Finite Difference Time Domain Method ” *IEEE Transactions on Antennas and Propagation* , Vol. 31, No. 11, November 1989
- [26] M. Zweeki, R.A. Abd-Alhameed, M.A. Mangoud, P.S. Excel and J.A. Vaul , “ Broadband Analysis of Finite Microstrip Patch Antenna Structure using FDTD ”, *11th International conference on Antennas and Propagation. Win, Manchester. U.K.*. 17-20 April 2001
- [27] A. Deb, J. Sekhar Roy, J. Ghosh and B. Gupta ,” Analysis of Triangular Patch Antenna Structure using hybrid FDTD Method” , *IEEE Transactions on Antennas and Propagation* , 2010
- [28] R Garg, P.Bhartiya , I.Bahl and A.Ittipiboon , *Microstrip Antenna Design Handbook*, Artech House, Boston, London, 2001.
- [29] Taflove , A., *Computational Electrodynamics : The Finite Difference Time Domain Method*, Artech House , Inc., 1995., *J.Compute. Phys.*, Vol.114 , 185-200, Oct. 1994
- [30] M. Bhardwaj and A. Kaur, “A Tri-band Microstrip Patch Antenna for Wireless Applications at 5.5, 6.3 and 6.8 GHz”, *International Journal of Advanced Research*

*in Electrical , Electronics and Instrumentation Engineering*, Vol. 1 , Issue 6 , June 2014

- [31] Y. S. H. Khraisat, M. M. Olaimat, “Comparison Between Rectangular and Triangular Patch Antennas Array,”*19<sup>th</sup> International Conference on Telecommunications( ICT 2012)* Vol 4,No.2; pp.1-5,2012
- [32] D.Shen , A. Lu , Y.Cui , F. Kuang , X. Zhang ,K.Wu and J.Yao ,” On the Channel Capacity of MIMO Rayleigh – Lognormal fading channel”, *ICMMT Proceedings* , 2010
- [33] C.Poongodi , K Dineshkumar , D.Deenadhayalan and Dr. A. Shanmugam ,”Capacity of Echleon , H-shaped , V-shaped and Printed dipole arrays in MIMO systems”, *IEEE*, 2011
- [34] L. Hanlen and A. Grant ,” Capacity Analysis of Correlated MIMO Channels”, *IEEE Transactions on Information Theory*, Vol. 58, NO. 11, November2012
- [35] A. K. Arya, M.V. Kartikeyan and A. Patnaik,” Defected Ground Structure in the perspective of Microstrip Antennas : A Review”, *Article in Frequenz-Berlin* , June 2010
- [36] C. Votis, G. Tatsis and Panos Kostarakis ,”Envelope Correlation Parameter Measurements in a MIMO Antenna Array Configuration”, *Int. J. Communications, Network and System Sciences*, 2010
- [37] M. Bouslama1, M.Traii1, A. Gharsallah and T.A. Denidni,”An Antenna Like Form ”Hand” of the Man on Five Bands WLAN/ Wimax / Hiper LAN2 / C Band Applications”, *Journal of Electromagnetic Analysis and Applications*, 2014
- [38] J. Malik, P C kalaria and M. V. Kartikeyan,”Complementary sierpinski Gasket Fractal antenna for dual-band WiMAX / WLAN (3.5/5.8 GHz) applications”, *International Journal of Microwave and Wireless Technologies*, 2013

- [39] C. Y. D .Sim, C.C. Chen and Y.L Lee "A Dual band Antenna Design for MIMO LTE Applications with Reduced Ground effects", *Wiley Online Library*, September 2015
- [40] S. Gupta and A. Kaur," A Review paper on Triangular Patch MIMO Antennas for Wireless Communications", *National Conference on Recent Innovations in Electronics , Electrical and Computer Engineering*, Vol 2. ,May 2015
- [41] S. Gupta , A. Agarwal and A. Kaur," FDTD Analysis of Microstrip Triangular Patch Antenna", *11<sup>th</sup> International Conference on Microwaves , Antennas, Propagation and Remote sensing (ICMARS)* , Dec. 2015
- [42] S. Gupta and A. Kaur," Design of Compact Triangular Microstrip Patch Fractal Antenna Array for MIMO Applications", *International Journal of Advances in Microwave Technology (IJAMT)* Vol.1, No.1, May 2016
- [43] A. Kaur, R. Khanna and M.V Kartikeyan , "A Stacked Sierpinski Gasket Fractal Antenna with a Defected Ground Structure for UWB/WLAN/ Radio Astronomy/ STM Link Applications", *Microwave and Optical Technology Letters* Vol. 57, No. 12, December 2015

# Paper

---

## ORIGINALITY REPORT

---

24%

SIMILARITY INDEX

11%

INTERNET SOURCES

15%

PUBLICATIONS

13%

STUDENT PAPERS

---

## PRIMARY SOURCES

---

1

[www.bandwidthers.org](http://www.bandwidthers.org)

Internet Source

1%

---

2

Submitted to Higher Education Commission  
Pakistan

Student Paper

1%

---

3

Zarbouti, Dimitra, George Tsoulos, and Dimitra  
Kaklamani. "Theory and Practice of MIMO  
Wireless Communication Systems", Electrical  
Engineering & Applied Signal Processing  
Series, 2006.

Publication

1%

---

4

Submitted to Lovely Professional University

Student Paper

1%

---

5

Submitted to Madan Mohan Malaviya  
University of Technology

Student Paper

1%

---

6

Submitted to Punjab Technical University

Student Paper

1%

---

7

Submitted to Dowling Catholic High School

Student Paper

1%